

Prognostic value and immune landscapes of anoikis-associated lncRNAs in lung adenocarcinoma

Bo Wu^{1,*}, Xiang Zhang^{1,*}, Nan Feng¹, Zishun Guo¹, Lu Gao², Zihua Wan^{2,*}, Wenxiong Zhang¹

¹Department of Thoracic Surgery, The Second Affiliated Hospital, Jiangxi Medical College, Nanchang University, Nanchang 330006, China

²Department of Thoracic Surgery, Baoding No.1 Central Hospital, Baoding 071000, China

*Equal contribution and co-first authorship

Correspondence to: Zihua Wan; email: wzh051014cy@163.com, <https://orcid.org/0009-0009-0797-3917>

Keywords: anoikis, lncRNAs, lung adenocarcinoma, overall survival, drug sensitivity

Received: May 9, 2023

Accepted: December 19, 2023

Published: February 5, 2024

Copyright: © 2024 Wu et al. This is an open access article distributed under the terms of the [Creative Commons Attribution License](https://creativecommons.org/licenses/by/4.0/) (CC BY 4.0), which permits unrestricted use, distribution, and reproduction in any medium, provided the original author and source are credited.

ABSTRACT

Background: Methods for predicting the outcome of lung adenocarcinoma (LUAD) in the clinic are limited. Anoikis is an important route to programmed cell death in LUAD, and the prognostic value of a model constructed with anoikis-related lncRNAs (ARlncRNAs) in LUAD is unclear.

Methods: Transcriptome and basic information for LUAD patients was obtained from the Cancer Genome Atlas. Coexpression and Cox regression analyses were utilized to identify prognostically significant ARlncRNAs and construct a prognostic signature. Furthermore, the signature was combined with clinical characteristics to create a nomogram. Finally, we performed principal component, enrichment, tumor mutation burden (TMB), tumor microenvironment (TME) and drug sensitivity analyses to evaluate the basic research and clinical merit of the signature.

Results: The prognostic signature developed with eleven ARlncRNAs can accurately predict that high-risk group patients have a worse prognosis, as proven by the receiver operating characteristic (ROC) curve (AUC: 0.718). Independent prognostic analyses indicated that the risk score is a significant independent prognostic element for LUAD (P<0.001). In the high-risk group, enrichment analysis demonstrated that glucose metabolism and DNA replication were the main enrichment pathways. TMB analysis indicated that the high-risk group had a high TMB (P<0.05). Drug sensitivity analyses can recognize drugs that are sensitive to different risk groups. Finally, 11 ARlncRNAs of this signature were verified by RT-qPCR analysis.

Conclusions: A novel prognostic signature developed with 11 ARlncRNAs can accurately predict the OS of LUAD patients and offer clinical guidance value for immunotherapy and chemotherapy treatment.

INTRODUCTION

Lung cancer (LC) is a carcinoma with high incidence and mortality rates [1]. Lung adenocarcinoma (LUAD) is an essential component of the pathobiological types of LC and is extremely heterogeneous [2]. With the continuous improvement of LUAD diagnostic and treatment protocols in the past decade, the survival rate has improved; however, the OS for LUAD patients is

still unsatisfactory [3]. Even worse, commonly used clinical assessment metrics (including TNM staging) cannot accurately predict LUAD prognosis. Presently, biomarkers are a sensitive indicator used to identify patient survival, and multibiomarker prognostic signatures have better predictive power than a single biomarker [4, 5]. Hence, determining reliable multi-biomarker prognostic features that predict the prognosis of LUAD patients is extremely important.

Programmed apoptosis is one of the major pathways of apoptosis in LUAD, in which anoikis plays an important role. Anoikis is a special type of programmed apoptosis that affects processes of cancer invasion and metastasis by disturbing mitochondria or automating cell surface death receptors, leading to apoptosis (Figure 1) [6, 7]. In recent years. Numerous studies have shown the discovery of anoikis as an important mechanism for cancer invasion and metastasis in gastric, breast, prostate and lung cancers [8–10]; for example, upregulation of the PDK4 gene leads to chemoresistance in LC and promotes cancer cell proliferation [10]. Despite the key role of anoikis genes in tumorigenesis and progression, the impact of anoikis on LUAD prognosis has rarely been studied. Moreover, long noncoding RNAs (lncRNAs) are engaged in cancer cell proliferation, migration and invasion processes [11]. Interestingly, lncRNAs have been reported to be closely correlated with anoikis in tumor cells. For example, the

anti-apoptotic effect of MRPL23-AS1 in cystic carcinoma of the salivary gland was observed *in vitro* [12]. In ovarian cancer, lncRNA HOTAIR regulates the anti-apoptotic ability of neoplastic cells by influencing EZH2 [13]. The above studies indicate that anoikis-related lncRNAs (ARlncRNAs) have an essential effect on the progression of cancer. To date, no research on ARlncRNAs in LUAD prognosis has been conducted. Therefore, it is necessary to investigate the association between ARlncRNAs and the OS of LUAD.

In the current study, we identified significantly prognostic ARlncRNAs for developing a novel prognostic signature in LUAD patients and then verified its predictive ability. Furthermore, we analyzed the sensitivity of different risk groups to common drugs, which offers clinical guidance value for immunotherapy and chemotherapy therapies.

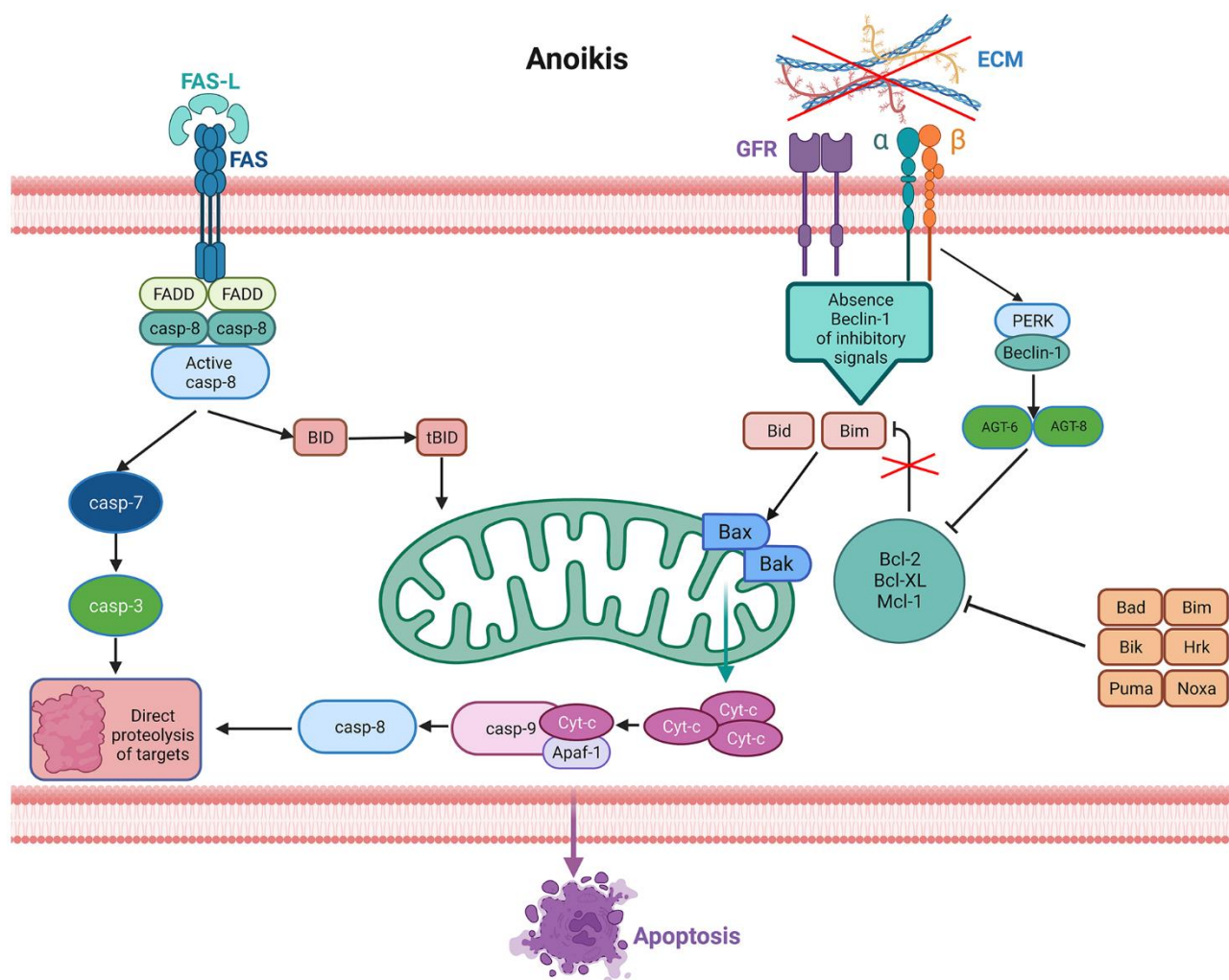


Figure 1. Signaling pathways activated in anoikis. Lack of the extracellular matrix (ECM) contact or improper ECM contact prevents the activation of pro-survival signals resulting in reduced anti-apoptotic pathways, thus activating anoikis from death receptors and mitochondria. Increased expression of extrinsic Fas receptors also activates the extrinsic pathway.

MATERIALS AND METHODS

Data acquisition

Clinical information and gene expression messages of 555 (506 LUAD samples) samples were downloaded from The Cancer Genome Atlas (TCGA) on September 3, 2022 (<https://portal.gdc.cancer.gov/>). Thirty-five LUAD samples with no survival time, survival condition or complete gene information were further excluded, and 471 patients with full clinical information were enrolled in the TCGA-LUAD cohort. Then, the cohort was randomly assigned to training (236 samples) and test (235 samples) cohorts at a ratio of 1:1 (Table 1). Construct a prognostic signature using the most valuable ARlncRNAs filtered from the training cohort data. TCGA-LUAD and test cohorts were utilized to test the predictability and clinical applicability of the signature. The data processing flow is detailed in Figure 2. Statistical analyses were performed with R software (version 4.2.3).

Identification of ARlncRNAs

Twenty-seven anoikis-related genes were acquired from the Molecular Signatures Database (MSigDB) [14]. Coexpression analysis in the “limma” R package was used to screen potential ARlncRNAs between anoikis-related genes and lncRNAs ($|R| > 0.4$; $P < 0.001$).

Development of the ARlncRNA prognostic signature

Combining significant ARlncRNAs with the clinical data of LUAD patients in the training group, univariate Cox regression analysis was undertaken to identify ARlncRNAs correlated with OS. Next, least absolute shrinkage and selection operator (LASSO) and multivariate Cox regression were utilized to recognize statistically significant prognostic ARlncRNAs. Finally, we constructed a novel prognostic signature developed with the above prognostic ARlncRNAs by multivariate Cox regression and calculated risk scores per patient. Risk Score = (Exp lncRNA1 \times β lncRNA1) + (Exp lncRNA2 \times β lncRNA2) + (Exp lncRNA3 \times β lncRNA3) + + (Exp lncRNA n \times β lncRNA n). The Exp represents was the expression of lncRNA and the β was the multivariate Cox regression analysis coefficient of lncRNA [15].

Evaluating the ARlncRNA prognostic signature and principal component analysis (PCA)

Patients were assigned to high- and low-risk cohorts according to the risk score. Survival status maps and ARlncRNA expression heatmaps of patients from the two risk groups were mapped with the “pheatmap” R

package. Kaplan–Meier curves were generated to compare the OS of the two risk groups with the “survival” R package. In addition, a receiver operating characteristic (ROC) curve was generated by the “timeROC” R package to assess the 1-, 3- and 5-year predictive capability of the prognostic signature and calculate the area under the curve (AUC). Finally, PCA was applied to estimate the capability of distinguishing between high- and low-risk patients via the “scatterplot3” and “limma” R packages [16].

Independent prognostic analysis

We investigated the prognostic value of the risk score and clinical characteristics in LUAD patients via univariate Cox regression. Meanwhile, correlation analysis was utilized for risk scores and the above clinical characteristics. The predictive accuracy of this signature was verified via the C-index and ROC curves. Then, a new nomogram model was developed with clinical characteristics and risk scores. A calibration curve is utilized to show the agreement between the predicted and actual outcomes. Decision curve analysis (DCA) was utilized to demonstrate the clinical applicability value of this model.

Clinical subgroup validation

The patients were assigned to different subgroups depending on clinicopathological characteristics in the training set. The subgroups were as follows: age (≤ 65 ; > 65), sex (female; male), stage (stage I-II; stage III-IV), T stage (T1-2; T3-4), and N stage (N0; N1-3). The OS of patients in the high- and low-risk groups was compared via subgroup analysis, and the aim was to determine the optimal range of application of the signature.

Gene set enrichment analysis (GSEA) and tumor mutation burden (TMB) analysis

Enrichment pathways for the two risk groups were examined by six different methods (kegg, go, reactome, biocarta, wikipathways, pid) in GSEA4.3.2 software, and $|NES| > 1$ and $FDR < 0.25$ were deemed reliable. TMB differences between the two risk groups were analyzed via the “maftools” R package [17]. Comparing the OS of patients in the high and low TMB groups via survival analysis.

Tumor microenvironment (TME) analysis

We calculated the level of infiltration of important immune cells in two risk groups by seven methods (quanted, timer, epic, ciberspot, ciberspotabs, mcpcounter and xcell) [18], and the outcome was then

Table 1. Clinicopathological characteristics of 471 LUAD patients in the TCGA database.

Characteristic	Total cohort	Training cohort	Test cohort	P-value
Total	471 (100%)	235 (50%)	236 (50%)	
Age				1.000
≤65	225 (47.77%)	111 (47.23%)	114 (48.31%)	
>65	236 (50.11%)	117 (49.79%)	119 (50.42%)	
Unknow	10 (2.12%)	7 (2.98%)	3 (1.27%)	
Gender				0.973
Female	256 (54.35%)	129 (54.89%)	127 (53.81%)	
Male	215 (45.65%)	106 (45.11%)	109 (46.19%)	
Stage				1.000
I	255 (54.14%)	129 (54.89%)	126 (53.39%)	
II	108 (22.93%)	52 (22.13%)	56 (23.73%)	
III	75 (15.92%)	35 (14.89%)	40 (16.95%)	
IV	25 (5.31%)	13 (5.53%)	12 (5.08%)	
Unknow	8 (1.70%)	6 (2.55%)	2 (0.85%)	
T stage				1.000
T1	160 (33.97%)	82 (34.89%)	78 (33.05%)	
T2	250 (53.08%)	122 (51.91%)	128 (54.24%)	
T3	39 (8.28%)	21 (8.94%)	18 (7.63%)	
T4	19 (4.03%)	7 (2.98%)	12 (5.08%)	
Unknow	3 (0.64%)	3 (1.28%)	0 (0.00%)	
N stage				1.000
N0	304 (64.54%)	147 (62.55%)	157 (66.53%)	
N1	87 (18.47%)	44 (18.72%)	43 (18.22%)	
N2	66 (14.01%)	31 (13.19%)	35 (14.83%)	
N3	2 (0.42%)	2 (0.85%)	0 (0.00%)	
Unknow	12 (2.55%)	11 (4.68%)	1 (0.42%)	
M stage				0.989
M0	318 (67.52%)	156 (66.38%)	162 (68.64%)	
M1	24 (5.10%)	12 (5.11%)	12 (5.08%)	
Unknow	129 (27.39%)	67 (28.51%)	62 (26.27%)	

Abbreviation: LUAD, Lung adenocarcinoma; TCGA, The Cancer Genome Atlas.

represented by heatmaps. In addition, immune cell infiltration rates were compared between the two risk group populations by Wilcoxon analysis. Finally, based on the data calculated by the ciberspotabs method, correlation analysis was utilized to evaluate the level of immune cell infiltration in correlation with the risk score.

Drug sensitivity analysis

Tumor immune dysfunction and exclusion (TIDE) data for LUAD were obtained via the website (<http://tide.dfci.harvard.edu/>) [19]. The relationship between risk scores and TIED was analyzed with the “ggpubr” and “limma” R packages ($P < 0.05$). Moreover, we analyzed the differentially expressed

immune checkpoint genes among the two risk groups. Finally, analyses of the sensitivity to common drugs by the “pRRophetic” R package for both high- and low-risk groups ($p\text{Filter} < 0.001$ and $\text{corPvalue} < 0.001$).

Immunohistochemistry staining and real-time quantitative polymerase chain reaction (RT-qPCR)

Immunohistochemical outcomes of differentially expressed anoikis-related genes between normal and tumor specimens were accessed through the Human Protein Atlas (HPA) database (<https://www.proteinatlas.org/>). In our study, human normal bronchial epithelium cells (BEAS-2B) and LUAD cells (NCI-

H1395, NCI-H1975) were purchased from the Cell Bank of the Chinese Academy of Sciences (Shanghai, China). RNA was obtained from tissues with TRIzol reagent (Invitrogen, USA). HiScript II (Vazyme, China) was utilized to synthesize cDNA by reverse transcription. Primers for RT-qPCR experiments of 11 ARlncRNAs are shown in Supplementary Table 1. β -actin was used as an internal reference. The expression levels of lncRNAs were calculated using $2^{-\Delta\Delta CT}$.

Availability of data and materials

The data sets used and/or analyzed during the current study are available from the corresponding author on reasonable request.

Consent for publication

All authors gave their consent for publication.

RESULTS

Identification of ARlncRNAs and development of the prognostic signature

The analysis process of this research is displayed in a flow chart (Figure 2). First, 2649 ARlncRNAs were screened by coexpression analysis of 16,876 lncRNAs associated with 27 anoikis-related genes. Then, co-expression analysis results between anoikis-related genes and ARlncRNAs expressed by a Sankey diagram

were obtained (Figure 3A). Next, combining the clinical data of patients in the training cohort, 148 ARlncRNAs associated with OS were identified among 2678 ARlncRNAs by univariate Cox regression analysis (Supplementary Table 2). Furthermore, 16 ARlncRNAs were significantly associated with prognosis from the above lncRNAs using LASSO regression analysis (Figure 3B, 3C). Finally, we identified 11 significant prognostic ARlncRNAs in LUAD patients via multivariate Cox regression analysis (Figure 3D). A correlation heatmap showed the relationship between 11 ARlncRNAs and anoikis-related genes (Figure 3E). The multivariate Cox regression analysis coefficient of ARlncRNAs is shown in Supplementary Table 3. Then, the risk scores of different patients will be counted according to the risk score formula, risk score = (Exp AL031602.2 \times -0.71045017820589) + (Exp BZW1-AS1 \times 0.432038348321673) + (Exp AC021087.1 \times -0.476411291926875) + (Exp GLIS2-AS1 \times -0.454008732783369) + (Exp ABCA9-AS1 \times 0.999706491359515) + (Exp AL606489.1 \times 0.259835252523394) + (Exp ZNF571-AS1 \times -0.34874860401809) + (Exp LINC02310 \times 0.75089202544965) + (Exp AL162632.3 \times 1.31557357109109) + (Exp LINC01117 \times 0.338762422003907) + (Exp HAS2-AS1 \times 0.775846321855369). The Exp was the expression of lncRNA in different patients. According to the median risk score, patients were divided into the high-risk and the low-risk groups. The results of the risk scores and risk groups for each patient in the total, training and test cohorts are shown in Supplementary Tables 4–6.

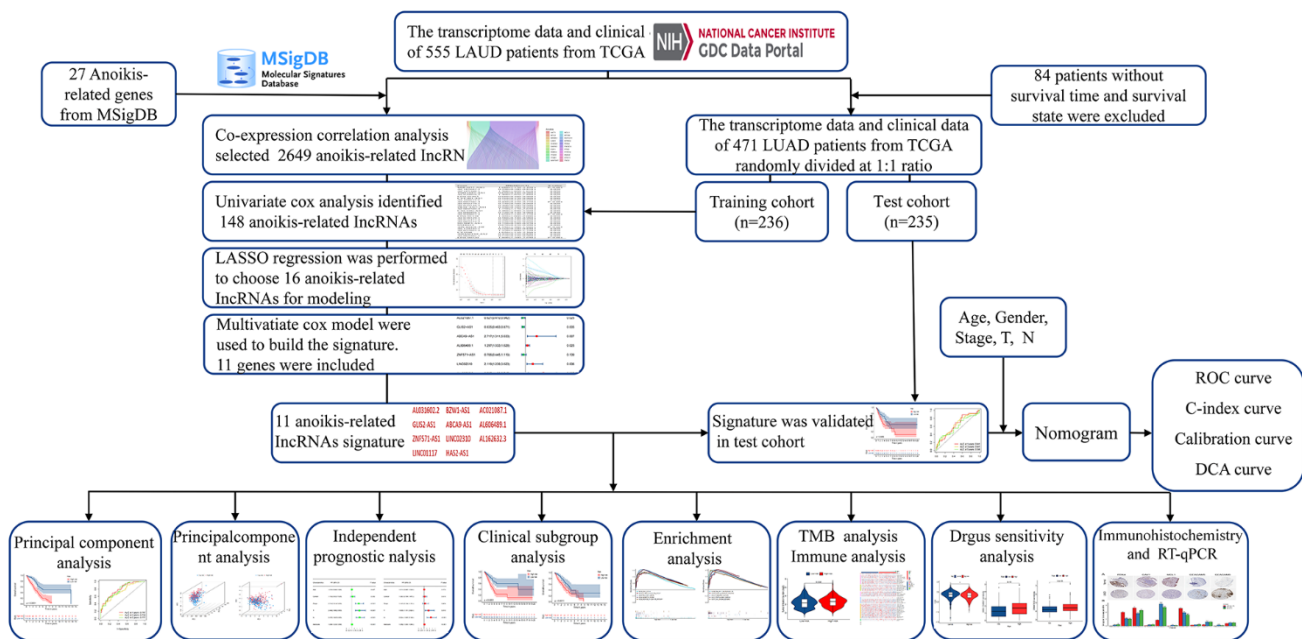


Figure 2. Overall flow diagram of the study.

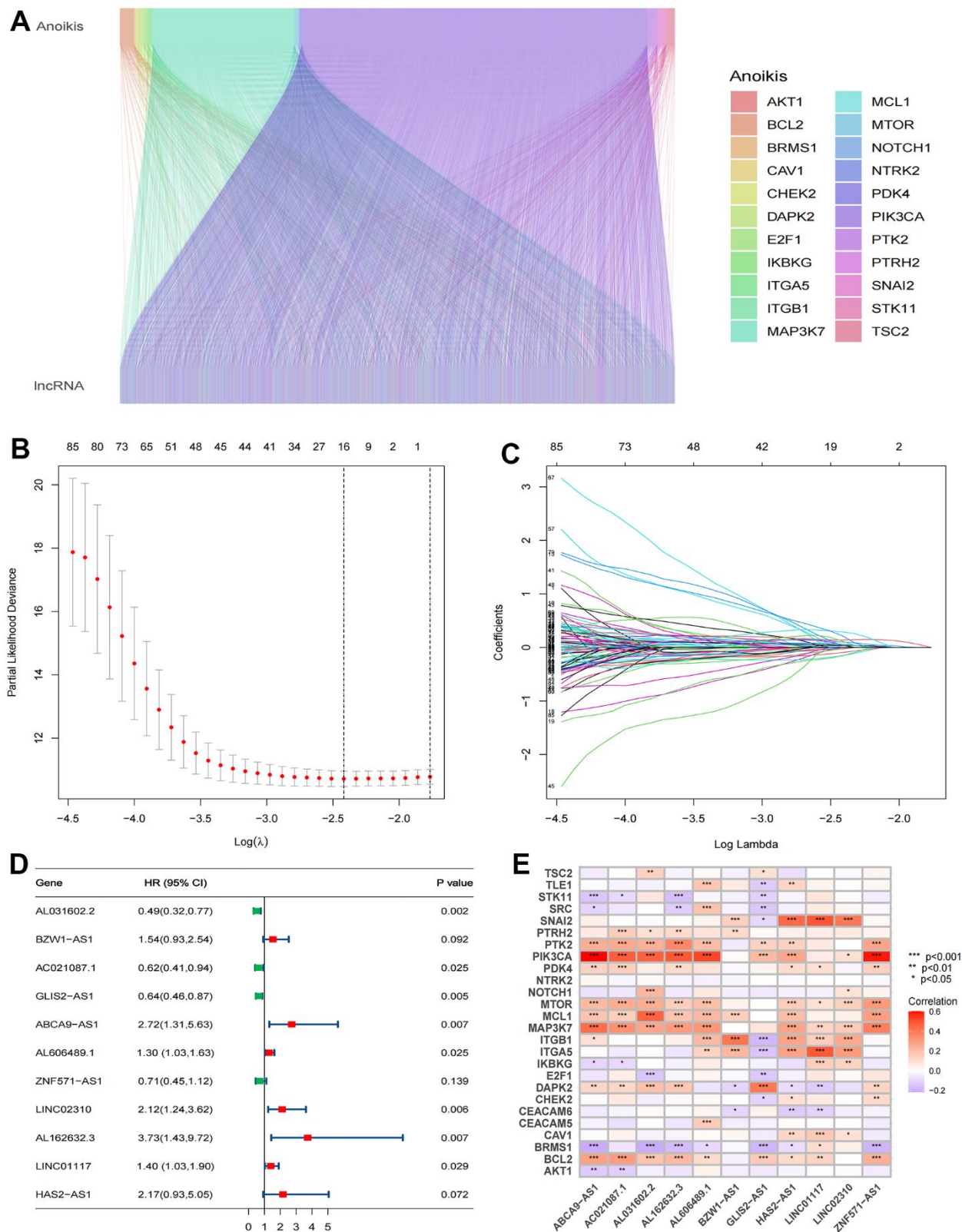


Figure 3. Identification of significant prognosis ARlncRNAs. (A) Sankey diagram depicting the relationships between 27 anoikis-related genes and ARlncRNAs co-expression. (B) LASSO Cox regression analysis revealed 85 ARlncRNAs based LASSO cross validation plot. (C) LASSO coefficient of 85 ARlncRNAs. (D) Forest plot showed different ARlncRNAs for high and low risk, with red representing high-risk lncRNAs and green representing low-risk ARlncRNAs. (E) Correlation heatmap showed the relationship between 11 ARlncRNAs and anoikis-related genes for the signature. Red represents positive correlations and blue represents negative correlations.

Evaluating the ARlncRNA prognostic signature and PCA

The TCGA-LUAD cohort was randomly assigned to training (236 samples) and test (235 samples) cohorts at a ratio of 1:1. We assigned the patients in each cohort to high- and low-risk cohorts according to the median risk score (Table 2), and the relationship between patients' risk scores and groups is shown by risk curves (Figure 4A). The risk survival status plot shows the poor survival of high-risk LUAD patients (Figure 4B). The AUCs for 1-, 3-, and 5-year OS were 0.718, 0.689, and 0.692 (entire cohort); 0.787, 0.738, and 0.777 (training cohort); and 0.641, 0.641, and 0.596 (test cohort, Figure 4C). Furthermore, a heatmap of the expression profile of 11 ARlncRNAs in the signature demonstrated that ARlncRNAs AL031602.2, AC021087.1, GLIS2-AS1, and ZNF571-AS1 were highly expressed in the low-risk group. Conversely, BZW1-AS1, ABCA9-AS1, AL606489.1, LINC02310, AL162632.3, LINC01117, and HAS2-AS1 were expressed at low levels (Figure 4D). Survival analysis revealed that high-risk group patients were correlated with worse OS and progression-free survival in all three cohorts (Figure 5A–5F). Finally, PCA results indicated that all genes, anoikis-related genes, and ARlncRNAs were unable to validly recognize high- and low-risk patients, and only risk ARlncRNAs could effectively recognize high- and low-risk patients (Figure 5G–5J).

Independent prognostic analysis

Cox regression analysis indicated that T stage ($P=0.010$), N stage and risk score ($P<0.001$) were independent prognostic factors (Table 3 and Supplementary Figure 1A, 1B). In addition, correlation analysis revealed that stage ($P=0.0019$), sex ($P=0.001$), T stage ($P=0.00072$), and N stage ($P<0.0001$) had significant relationships with risk scores, while age ($P=0.88$) was not significantly related to risk scores (Supplementary Figure 1C–1G). Finally, we developed a new nomogram with risk scores and clinical characteristics for predicting the OS of LUAD patients at 1, 3 and 5 years (Figure 6A). The ROC curve results showed that the risk score (AUC: 0.718) had better predictive ability than age (0.543), sex (0.598), stage (0.614), T stage (0.608) and N stage (0.619) (Figure 6B), which was also indicated by the C-index curves (Figure 6C). The nomogram with risk score had more accurate predictive prognostic ability compared to no risk scores (AUC: 0.737 vs. 0.694, Figure 6B), which precisely forecasted the OS of patients in the test cohort (Supplementary Figure 2). Calibration curves show the agreement between the predicted and actual outcomes, and DCA demonstrated the clinical applicability value of this model (Figure 6D, 6E).

Clinical subgroup validation

The heatmap shows the expression of 11 ARlncRNAs in different clinical subgroups (Supplementary Figure 3A). To determine the optimal range of application of this signature, survival analysis was performed for the two risk groups in the subgroups. Kaplan–Meier curves showed that the high-risk group was related to worse OS in all subgroups (Supplementary Figure 4B–4F). Moreover, this difference was more significant in the age ≤ 65 , stage I-II, T1-2 and N0 subgroups ($P<0.001$).

GSEA and TMB analysis

Enrichment results for six different pathway bases showed that glucose metabolism and DNA replication were the main enrichment pathways in the high-risk group. Notably, there was no significant enrichment pathway in the low-risk group (Figure 7). Depending on the results of the maftools algorithm, waterfall plots show that the mutation frequency of most genes was markedly increased in the high-risk group, such as TP53, TTN, MUC16, etc. (Figure 8A, 8B). Furthermore, the high-risk group was significantly linked to a high TMB. (Figure 8C). Survival analysis based on TMB results showed that the high TMB group had good OS compared to the low TMB group (Figure 8D, 8E).

Tumor microenvironment analysis

Most immune cell infiltration levels were noticeably dissimilar in the two risk groups, as shown by the heatmap (Figure 9A). Wilcoxon analysis showed significantly lower infiltration rates of activated myeloid dendritic cells and B-cell memory in the high-risk group. In contrast, the infiltration rates of M0 macrophages and CD8+ T cells were significantly higher (Figure 9B). Moreover, immune function analysis demonstrated that 4 (HLA, MHC class I, parainflammation, type II IFN response) immune function pathways were significantly different between the two risk groups (Figure 9C).

Immunotherapy and chemotherapy sensitivity

According to the results of the TIED algorithm, tumor cells in the low-risk group appeared more easily to be immune escapees (Figure 10A). Gene expression analyses of immune checkpoints indicated that the highly expressed immune checkpoint genes were TNFRSF25, LGALS9, CD160, IDO2, TNFRSF14, TNFSF14, TNFSF15, CD40LG, CD200R1 and ADORA2A in the low-risk group and CD70, CD276 and TNFSF4 in the high-risk group (Figure 10B). Drug sensitivity analyses revealed that low-risk group patients had 6 sensitive drugs, and the pharma-

Table 2. Clinicopathological characteristics of LUAD patients in two risk groups.

Characteristic	High-risk group	Low-risk group
Total	237 (50%)	234 (50%)
Age		
≤65	111 (46.84%)	114 (48.72%)
>65	121 (51.05%)	115 (49.15%)
Unknow	5 (2.11%)	5 (2.14%)
Gender		
Female	115 (48.52%)	141 (60.26%)
Male	122 (51.48%)	93 (39.74%)
Stage		
I	104 (43.88%)	151 (64.53%)
II	66 (27.85%)	42 (17.95%)
III	45 (18.99%)	30 (12.82%)
IV	18 (7.59%)	7 (2.99%)
Unknow	4 (1.69%)	4 (1.71%)
T stage		
T1	59 (24.89%)	101 (43.16%)
T2	138 (58.23%)	112 (47.86%)
T3	28 (11.81%)	11 (4.70%)
T4	10 (4.22%)	9 (3.85%)
Unknow	2 (0.84%)	1 (0.43%)
N stage		
N0	133 (56.12%)	171 (73.08%)
N1	56 (23.63%)	31 (13.25%)
N2	41 (17.30%)	25 (10.68%)
N3	0 (0.00%)	2 (0.85%)
Unknow	7 (2.95%)	5 (2.14%)
M stage		
M0	161 (67.93%)	157 (67.09%)
M1	17 (7.17%)	7 (2.99%)
Unknow	59 (24.89%)	70 (29.91%)

Abbreviation: LUAD, Lung adenocarcinoma.

ological action of these drugs is mainly by interdicting the PI3K/MTOR and ERK MAPK signaling pathways (Supplementary Table 7). The high-risk group had 59 sensitive drugs, and the pharmacological effect was mainly mediated by blocking mitosis and the IGF1R signaling pathway (Supplementary Table 8 and Figure 10C–10K).

Immunohistochemistry staining and RT–qPCR

Protein expression maps of differentially expressed anoikis-associated genes in the HPA database showed that PDK4, CAV1, and MCL1 were expressed at relatively low levels in LUAD. In contrast, CEACAM5 and CEACAM6 were relatively highly expressed

(Supplementary Figure 4A). Primers for RT–qPCR experiments of 11 ARlncRNAs are shown in Supplementary Table 1. RT–qPCR measurements showed significant differential expression of the above 11 ARlncRNAs in human normal bronchial epithelium cells (BEAS-2B) and LUAD cells (Supplementary Figure 4B). These results are in good agreement with the outcome of our analyses in the TCGA database.

DISCUSSION

LUAD is the most predominant pathobiological type of LC and is highly heterogeneous [1, 2]. With the continuous improvement of LUAD diagnostic and treatment protocols in the past decade, the OS for

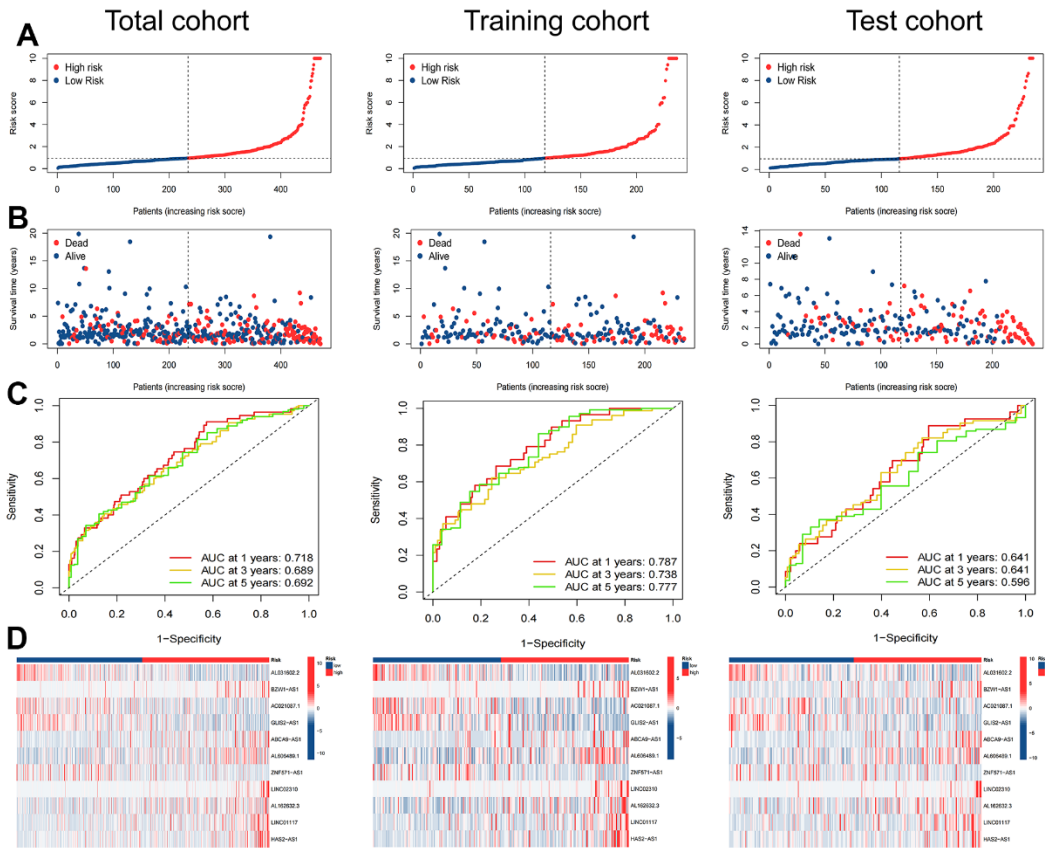


Figure 4. Evaluation of the ARlncRNA prognostic signature in the total, training and test cohorts. (A) Risk score distribution of patients with LUAD based on ARlncRNAs. (B) Scatter plots showed the association between the overall survival and the risk score distribution. (C) 1-, 3-, and 5-years overall survival area under the ROC curve of the signature. (D) Heatmap represented the expression of 11 ARlncRNAs involved in the signature.

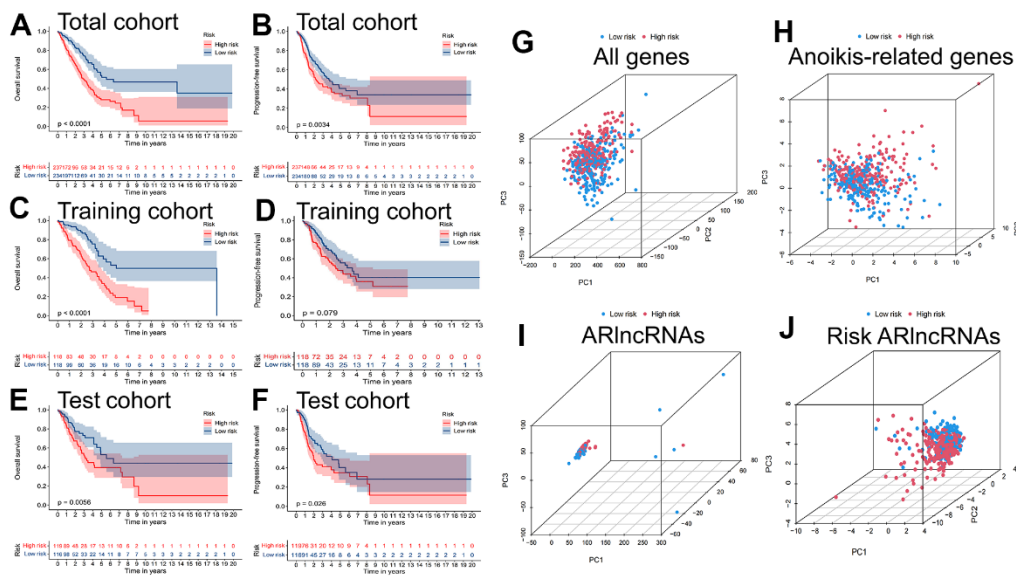


Figure 5. Survival and PCA analysis of the prognostic signature. Kaplan-Meier curves to compare the overall survival and progression-free survival of high-risk group and low-risk group in the (A, B) total, (C, D) training and (E, F) test cohort. Principal component analysis (PCA) based on (G) All genes, (H) Anoikis-related genes, (I) ARlncRNAs, and (J) Risk ARlncRNAs.

Table 3. Univariate and multivariate Cox regression analysis based on risk factors (Training cohort).

Characteristic	Univariate analysis			Multivariate analysis		
	HR	HR (95% CI)	P-value	HR	HR (95% CI)	P-value
Age	1.01	(0.99, 1.03)	0.227	1.010	(1.00, 1.03)	0.173
Gender	1.16	(0.85, 1.56)	0.350	1.080	(0.79, 1.47)	0.618
Stage	2.31	(1.67, 3.20)	<0.001	1.160	(0.75, 1.79)	0.498
T	2.44	(1.66, 3.58)	<0.001	1.800	(1.15, 2.82)	0.010
N	2.47	(1.82, 3.35)	<0.001	2.220	(1.55, 3.20)	<0.001
Risk Score	1.05	(1.03, 1.06)	<0.001	1.050	(1.04, 1.07)	<0.001

Abbreviations: CI, Confidence interval; HR, Hazard ratio.

LUAD patients is still unsatisfactory [3]. Traditional TNM staging and clinical prediction models cannot effectively predict the OS of LUAD and guide therapy [5]. It is urgent to discover a new predictive model. anoikis is a special type of programmed apoptosis that occurs when cancer cells are separated from the extra-cellular matrix (ECM), which influences tumorigenesis,

metastasis and invasion [9]. Recently, lncRNAs have been reported to be closely correlated with anoikis in tumor cells [20]. Therefore, exploring the effect of ARlncRNAs on the prognosis of LUAD is necessary. The study identified significantly prognostic ARlncRNAs to develop a novel prognostic signature that can validly predict the OS of LUAD. In the

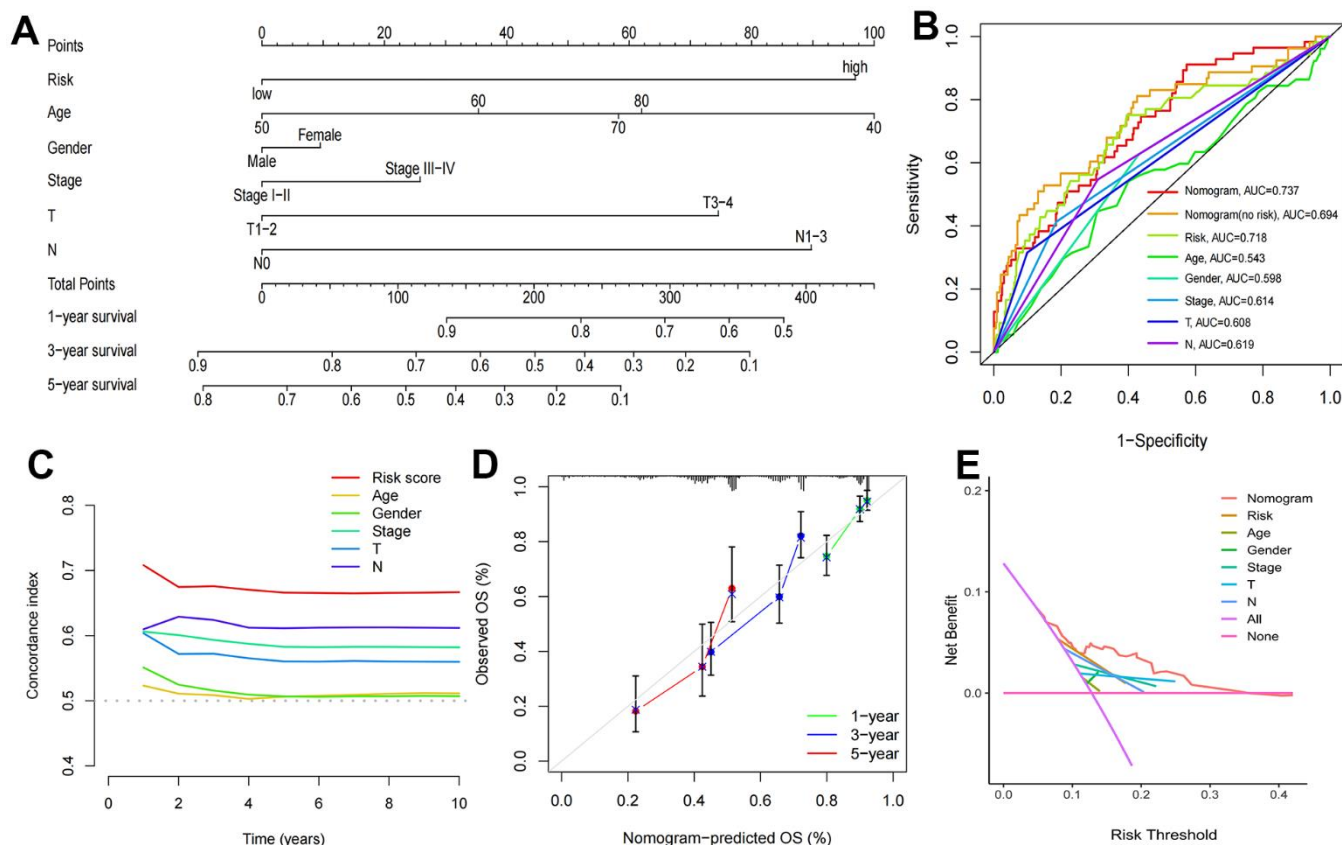


Figure 6. Construction of nomogram and validation of its predictive ability. (A) The nomogram for predicting the overall survival of patients with LUAD at 1-, 3-, and 5- years. **(B)** ROC curves for the risk score and other clinical characteristics to predict the overall survival rates of patients with LUAD. **(C)** C-Index curve for the risk score and other clinical characteristics. **(D)** The calibration curve for evaluating the nomogram. **(E)** DCA curve of the nomogram.

high-risk group, enrichment analysis demonstrated that glucose metabolism and DNA replication were the main enrichment pathways. Patients in the high-risk group were immunosuppressed and had a high TMB. Two risk groups with different sensitivities to immunotherapy and different chemotherapeutic drugs.

We developed a novel prognostic signature with accurate predictive ability based on 11 ARlncRNAs. Using lncRNAs to construct prognostic signatures is widely used in colorectal, esophageal and breast cancer [21]. The results of this study are similar to theirs. Poorer prognosis in the high-risk group and prognostic features accurately predict patient prognosis. To more accurately predict LUAD prognosis. We combined the signature with clinical characteristics to create a new nomogram, which has more accurate predictive ability than the nomogram without risk scores (AUC: 0.737 vs. 0.694). Since we incorporated risk scores with high predictive prognostic power, our model also has advantages over traditional TNM stage (AUC: 0.737 vs. 0.614), and has better predictive ability than other existing models [22, 23]. Two ARlncRNAs in the signature have been reported in the relevant literature. Zhao et al. demonstrated that LINC02310 significantly promoted the growth and proliferation of LUAD [24]. Experiments showed that HAS2-AS1 overexpression strongly reduced breast cancer cell viability, migration and invasion [25]. This is consistent with our study results. Mechanisms of action for other ARlncRNAs

still need to be further explored. RT-qPCR also confirmed the significant differential expression of the above 11 ARlncRNAs in normal and tumor cells.

GSEA showed that glucose metabolism and DNA replication were the main enrichment pathways in the high-risk group. The EGFR signaling pathway enhances SCAP N-glycosylation to deactivate SREBP-1 by promoting glucose uptake, and SREBP-1 can promote the progressive metastasis of cancer [26]. The DNA replication process plays a vital role in cell division and cancer progression [27]. The TME is involved in tumorigenesis, growth and metastasis [28]. The immune hypothesis suggests that fewer immune cancer cells in immunocompetent hosts evade antitumor immune responses. This may lead to an increase in immunosuppressive cells and a decrease in immunoreactive cells [29]. The study's immune infiltration analyses revealed that the high-risk group had higher NK cell infiltration but lower mast cell and helper T-cell infiltration than the low-risk group. This high level of immunosuppression and poor immune responsiveness may contribute to the poor prognosis of high-risk patients. Immune function analysis showed differences in HLA, MHC class I, parainflammatory, and type II IFN responses between the two risk groups. Previous studies have demonstrated that decreased expression of HLA protein on the surface of cancer cells is an important mechanism of immune escape of tumor cells [30]. Furthermore, TMB is usually

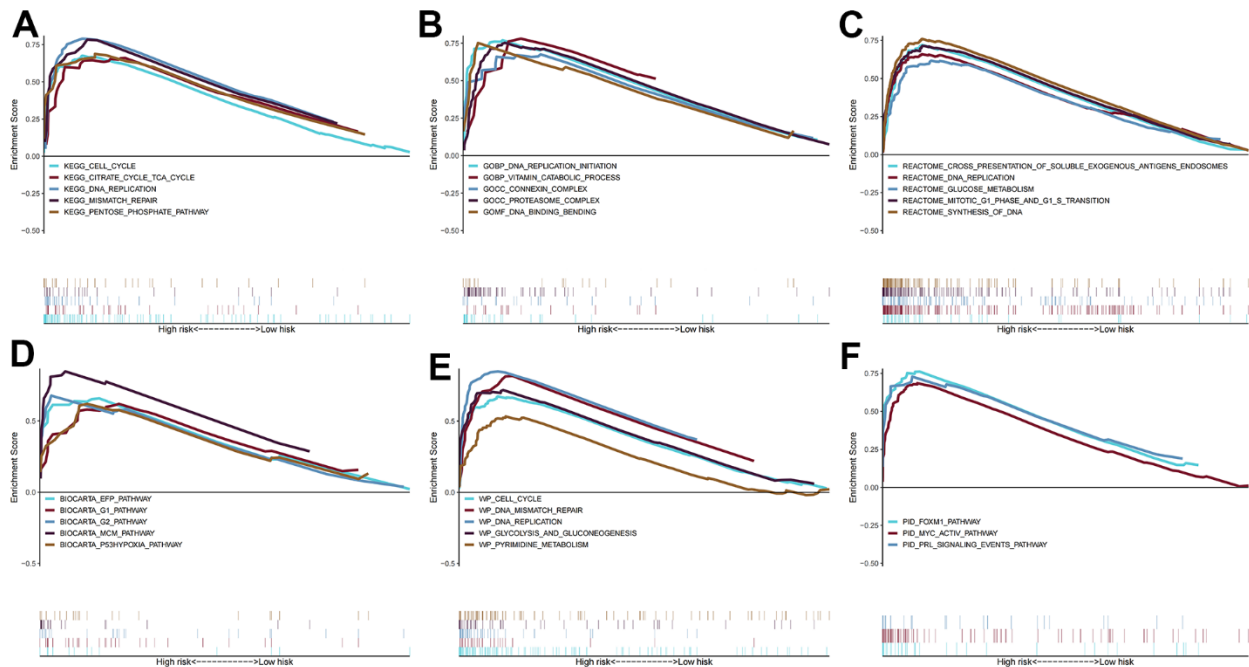


Figure 7. Gene set enrichment analysis. The pathways of (A) KEGG, (B) GO, (C) BIOCARTA, (D) REACTOME, (E) WIKIPATHWAYS, and (F) PID enriched in the low- and high- risk group.

employed as a predictive indicator for immunotherapy in urothelial, lung and head and neck squamous cell cancers [31]. Our study found that the top two significantly different mutated genes between the high and low risk groups were TP53 and TTN. TP53 is the most mutable tumor suppressor gene, and its mutation not only increases the chance of carcinogenesis but also decreases antitumor activity [32]. TTN is also involved in the progression of many cancers. Jia et al. found that TTN regulates CDK5 through miR-142-5p to promote migration and invasion in LUAD [33]. This study found that patients with high TMB have a better prognosis. Studies have shown that patients may benefit more from immunotherapy with higher TMB [34]. However, in lung cancer patients with EGFR mutations, a higher TMB is associated with a poorer response to targeted therapy [35]. Additionally, for surgically resected early-

stage lung cancer patients, a higher TMB is correlated with longer survival, potentially allowing for the avoidance of postoperative adjuvant chemotherapy [36]. Our findings reconfirmed that the TMB affects the prognosis of patients with LUAD, which may provide guidance for immunotherapy, targeted therapy and chemotherapy.

TIDE plays an essential role in tumor progression and is an essential tool for predicting the effectiveness of immunotherapy in oncology. Studies have demonstrated that oncology patients with lower TIDE can benefit significantly from immunotherapy [37]. Our study found lower TIDE scores in the high-risk group, which suggests that these patients are more sensitive to immunotherapy. Thus, we further explored the distinction in immunotherapy response among the two

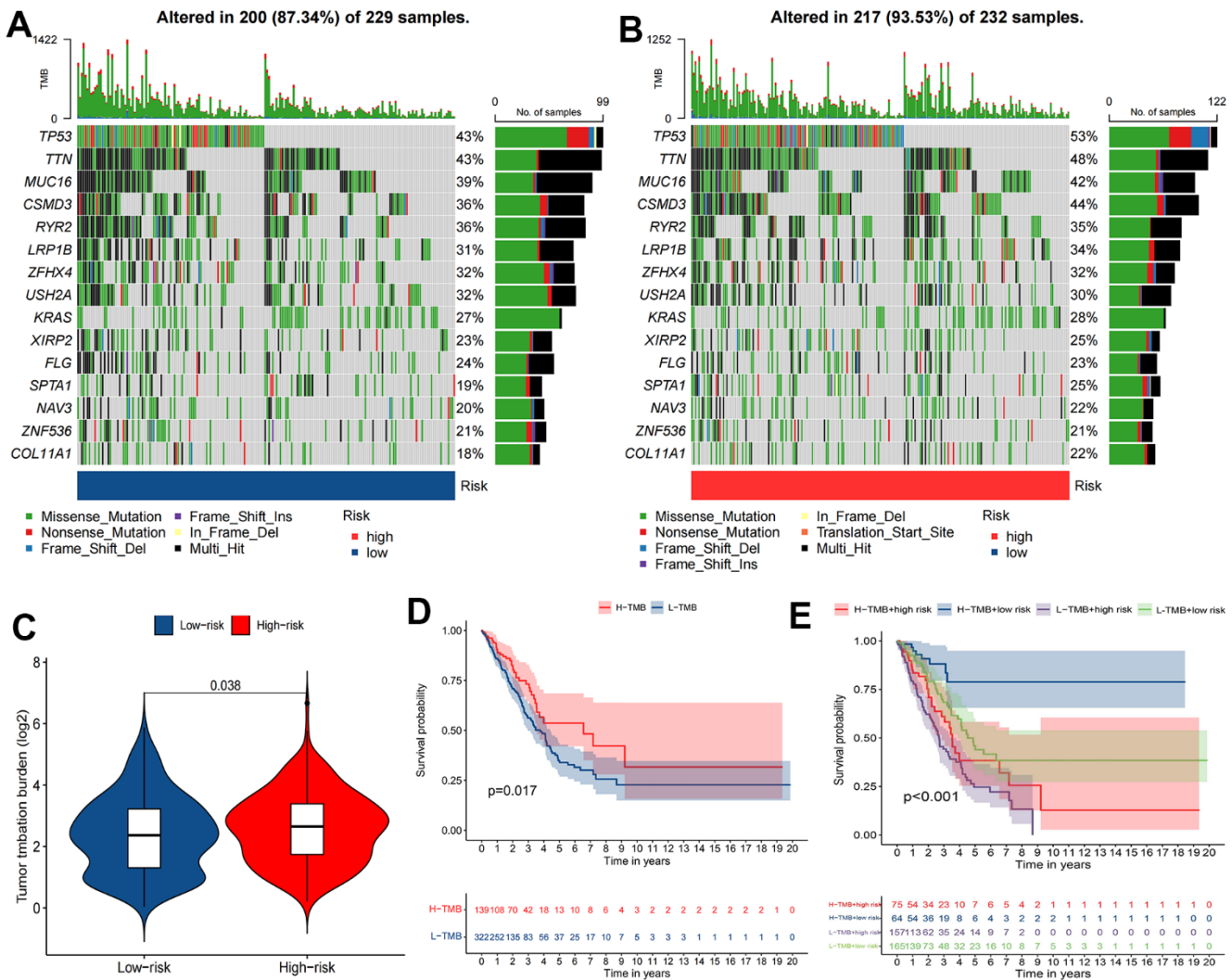


Figure 8. The relationship between TMB and the signature. (A, B) Waterfall plot revealed the top 15 mutation genes in LUAD for the two risk groups. **(C)** Differential TMB between two risk groups in LUAD. **(D, E)** Kaplan-Meier survival curves for the high and low TMB groups and a combined TMB-risk survival curve.

risk groups of LUAD patients. The expression of immune checkpoint genes was analyzed, and the results showed 12 differentially expressed immune checkpoint genes, 6 of which were highly expressed in high-risk populations, and the rest were highly expressed in low-risk populations. These genes could be potential targets for immunotherapy [38]. Furthermore, we collected common chemotherapeutic drugs, and the sensitivities of the two risk groups to these drugs were analyzed via the pRRophetic algorithm [39]. Our results revealed that the sensitive drugs in the high-risk group of patients mainly blocked mitosis and the IGF1R signaling pathway but were resistant to the PI3K/MTOR and ERK MAPK signaling pathways. This indicated that this prognostic signature can predict chemotherapy drug sensitivity in LUAD patients. Overall, the ARlncRNA prognostic signature can offer clinical guidance value for immunotherapy and chemotherapy treatment.

The strengths of this study are as follows: This study is the first to analyze the relationship between ARlncRNAs and prognosis of LUAD patients and attempts to use ARlncRNAs as a biological prognosticator for predicting LUAD patients. Second, the model performed better in predicting patient prognosis compared with the traditional model, which indicates the potential clinical application of ARlncRNAs in LUAD prognosis prediction. Third, this

study pioneered the use of six gene enrichment analysis methods and searched for common metabolic pathways, providing a deep understanding of the intrinsic mechanisms of LUAD. Fourth, immune function, immune checkpoint and TIED analysis revealed differences in the immune landscape between high and low risk groups, providing new ideas for future studies, and finally, validated using cell lines, which lends credibility to the study. Nonetheless, some limitations of this study should be mentioned. First, LUAD patients from a single data source TCGA database. Second, the molecular mechanism of ARlncRNAs in the OS of LUAD is unclear and will be explored in future studies.

CONCLUSIONS

We developed a novel signature with 11 ARlncRNAs that can precisely predict the OS of LUAD patients. Nomograms with risk scores have more accurate predictive prognostic power than those without risk scores. The high-risk group had gene enrichment mainly in glucose metabolism and DNA replication pathways, low immune response and high TMB. The novel signature can provide guidance for clinical immunotherapy and chemotherapy treatment. Due to these shortcomings, our study requires basic experimentation to discover the molecular mechanisms of ARlncRNAs in LUAD, and the selection of relevant sensitive drugs must be confirmed by clinical use.

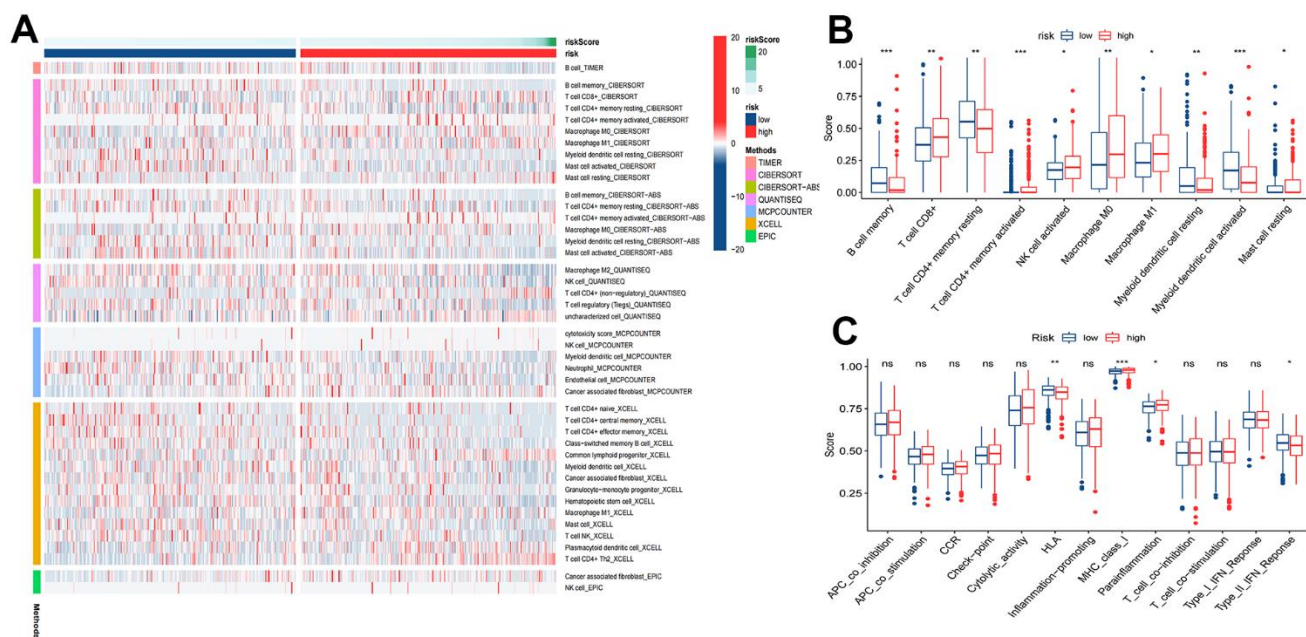


Figure 9. Tumor immune microenvironment analysis. (A) Heatmap for immune responses based on TIMER, CIBERSORT, CIBERSORT-ABS, QUANTISEQ, MCPOUNTER, XCELL, and EPIC algorithms among high and low risk groups. (B) ssGSEA algorithm shows immune cells scores between the two risk groups. (C) ssGSEA algorithm shows immune functions scores between the two risk groups. *P<0.05; **P<0.01; ***P<0.001.

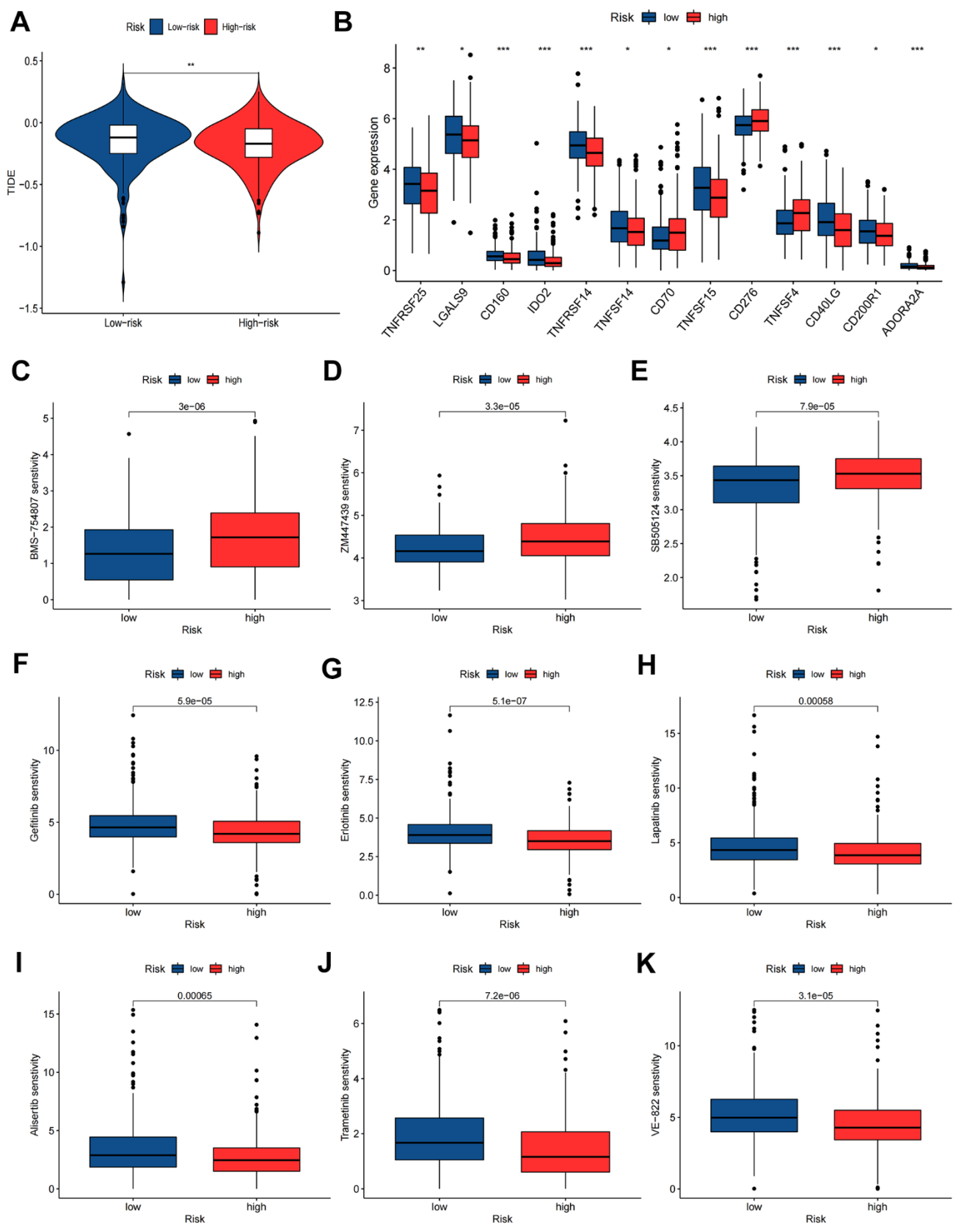


Figure 10. Immunotherapy and chemotherapy sensitivity. (A) Tumor immune dysfunction and exclusion (TIDE) algorithm analysis for the high-risk and low-risk groups. (B) Immune checkpoint genes expression level between high-risk and low-risk groups. (C-K) Chemosensitivity difference between high-risk and low-risk groups. * $P < 0.05$; ** $P < 0.01$; *** $P < 0.001$.

Abbreviations

AUC: Area under curve; ARlncRNAs: Anoikis-related lncRNAs; CI: Confidence interval; C-index: Concordance index; DCA: Decision curve analysis; ECM: The extracellular matrix; GSEA: Gene set enrichment analysis; HPA: The Human Protein Atlas; HR: Hazard ratio; LASSO: Least absolute shrinkage and selection operator; LC: Lung cancer; TCGA: The Cancer Genome Atlas database; LncRNAs: Long noncoding RNAs; LUAD: Lung adenocarcinoma; OS: Overall survival; PCA: Principal component analysis; ROC: Receiver operating characteristic curve; TIDE: The tumor immune dysfunction and exclusion; TMB: Tumor mutation burden; TME: Tumor microenvironment.

AUTHOR CONTRIBUTIONS

Zhihua Wan had full access to all of the data in the manuscript and takes responsibility for the integrity of the data and the accuracy of the data analysis. All authors read and approved the final manuscript. Concept and design: All authors. Acquisition, analysis, or interpretation of data: All authors. Drafting of the manuscript: Bo Wu, Xiang Zhang, Nan Feng Zishun Guo and Lu Gao. Experiments: Bo Wu, Xiang Zhang, Nan Feng Zishun Guo and Lu Gao. Statistical analysis: Bo Wu, Zhihua Wan and Wenxiong Zhang. Critical revision of the manuscript for important intellectual content: Bo Wu, Zhihua Wan and Wenxiong Zhang. Supervision: Bo Wu, Zhihua Wan and Wenxiong Zhang.

ACKNOWLEDGMENTS

The authors appreciate all the public health workers who participated in the TCGA database and R language developers.

CONFLICTS OF INTEREST

The authors declare that they have no conflicts of interest.

ETHICAL STATEMENT

The data of this paper is extracted from TCGA database, where it is publicly available and unrestricted re-use is permitted via an open license. This study is exempt from ethical approval by default.

FUNDING

This study was supported by National Natural Science Foundation of China (NSFC, Grant number: 81560345) and Natural Science Foundation of Jiangxi Province (Grant number: 20212BAB206050). The funding had

no role in the design and conduct of the study; collection, management, analysis, and interpretation of the data; preparation, review, or approval of the manuscript; and decision to submit the manuscript for publication.

REFERENCES

1. Siegel RL, Miller KD, Wagle NS, Jemal A. Cancer statistics, 2023. *CA Cancer J Clin.* 2023; 73:17–48. <https://doi.org/10.3322/caac.21763> PMID:36633525
2. Russell PA, Wainer Z, Wright GM, Daniels M, Conron M, Williams RA. Does lung adenocarcinoma subtype predict patient survival?: A clinicopathologic study based on the new International Association for the Study of Lung Cancer/American Thoracic Society/European Respiratory Society international multidisciplinary lung adenocarcinoma classification. *J Thorac Oncol.* 2011; 6:1496–504. <https://doi.org/10.1097/JTO.0b013e318221f701> PMID:21642859
3. Duffy SW, Field JK. Mortality Reduction with Low-Dose CT Screening for Lung Cancer. *N Engl J Med.* 2020; 382:572–3. <https://doi.org/10.1056/NEJMe1916361> PMID:31995680
4. Roper N, Brown AL, Wei JS, Pack S, Trindade C, Kim C, Restifo O, Gao S, Sindiri S, Mehrabadi F, El Meskini R, Ohler ZW, Maity TK, et al. Clonal Evolution and Heterogeneity of Osimertinib Acquired Resistance Mechanisms in EGFR Mutant Lung Cancer. *Cell Rep Med.* 2020; 1:100007. <https://doi.org/10.1016/j.xcrm.2020.100007> PMID:32483558
5. Yao J, Chen X, Liu X, Li R, Zhou X, Qu Y. Characterization of a ferroptosis and iron-metabolism related lncRNA signature in lung adenocarcinoma. *Cancer Cell Int.* 2021; 21:340. <https://doi.org/10.1186/s12935-021-02027-2> PMID:34217273
6. Raeisi M, Zehtabi M, Velaei K, Fayyazpour P, Aghaei N, Mehdizadeh A. Anoikis in cancer: The role of lipid signaling. *Cell Biol Int.* 2022; 46:1717–28. <https://doi.org/10.1002/cbin.11896> PMID:36030535
7. Chen S, Gu J, Zhang Q, Hu Y, Ge Y. Development of Biomarker Signatures Associated with Anoikis to Predict Prognosis in Endometrial Carcinoma Patients. *J Oncol.* 2021; 2021:3375297. <https://doi.org/10.1155/2021/3375297> PMID:34992654
8. Zhang T, Wang B, Su F, Gu B, Xiang L, Gao L, Zheng P, Li

- XM, Chen H. TCF7L2 promotes anoikis resistance and metastasis of gastric cancer by transcriptionally activating PLAUR. *Int J Biol Sci.* 2022; 18:4560–77. <https://doi.org/10.7150/ijbs.69933> PMID:35864968
9. Zhou X, Li L, Guo X, Zhang C, Du Y, Li T, Tong K, Zhu C, Wang Z. HBXIP induces anoikis resistance by forming a reciprocal feedback loop with Nrf2 to maintain redox homeostasis and stabilize Prdx1 in breast cancer. *NPJ Breast Cancer.* 2022; 8:7. <https://doi.org/10.1038/s41523-021-00374-x> PMID:35027562
 10. Sousa B, Pereira J, Marques R, Grilo LF, Pereira SP, Sardão VA, Schmitt F, Oliveira PJ, Paredes J. P-cadherin induces anoikis-resistance of matrix-detached breast cancer cells by promoting pentose phosphate pathway and decreasing oxidative stress. *Biochim Biophys Acta Mol Basis Dis.* 2020; 1866:165964. <https://doi.org/10.1016/j.bbadis.2020.165964> PMID:32920119
 11. Bhan A, Soleimani M, Mandal SS. Long Noncoding RNA and Cancer: A New Paradigm. *Cancer Res.* 2017; 77:3965–81. <https://doi.org/10.1158/0008-5472.CAN-16-2634> PMID:28701486
 12. Li YR, Fu M, Song YQ, Li SL, Ge XY. Long non-coding RNA MRPL23-AS1 suppresses anoikis in salivary adenoid cystic carcinoma *in vitro*. *Oral Dis.* 2023; 29:1588–601. <https://doi.org/10.1111/odi.14156> PMID:35175670
 13. Dai ZY, Jin SM, Luo HQ, Leng HL, Fang JD. LncRNA HOTAIR regulates anoikis-resistance capacity and spheroid formation of ovarian cancer cells by recruiting EZH2 and influencing H3K27 methylation. *Neoplasma.* 2021; 68:509–18. https://doi.org/10.4149/neo_2021_201112N1212 PMID:33502891
 14. Sun Z, Zhao Y, Wei Y, Ding X, Tan C, Wang C. Identification and validation of an anoikis-associated gene signature to predict clinical character, stemness, IDH mutation, and immune infiltration in glioblastoma. *Front Immunol.* 2022; 13:939523. <https://doi.org/10.3389/fimmu.2022.939523> PMID:36091049
 15. Tang Y, Xu L, Ren Y, Li Y, Yuan F, Cao M, Zhang Y, Deng M, Yao Z. Identification and Validation of a Prognostic Model Based on Three MVI-Related Genes in Hepatocellular Carcinoma. *Int J Biol Sci.* 2022; 18:261–75. <https://doi.org/10.7150/ijbs.66536> PMID:34975331
 16. Lv W, Tan Y, Zhou X, Zhang Q, Zhang J, Wu Y. Landscape of prognosis and immunotherapy responsiveness under tumor glycosylation-related lncRNA patterns in breast cancer. *Front Immunol.* 2022; 13:989928. <https://doi.org/10.3389/fimmu.2022.989928> PMID:36189319
 17. Zhang HC, Deng SH, Pi YN, Guo JN, Xi H, Shi X, Yang XF, Zhang BM, Xue WN, Cui BB, Liu YL. Identification and Validation in a Novel Quantification System of Ferroptosis Patterns for the Prediction of Prognosis and Immunotherapy Response in Left- and Right-Sided Colon Cancer. *Front Immunol.* 2022; 13:855849. <https://doi.org/10.3389/fimmu.2022.855849> PMID:35444656
 18. Wang Y, Lu G, Xue X, Xie M, Wang Z, Ma Z, Feng Y, Shao C, Duan H, Pan M, Ding P, Li X, Han J, Yan X. Characterization and validation of a ferroptosis-related lncRNA signature as a novel prognostic model for lung adenocarcinoma in tumor microenvironment. *Front Immunol.* 2022; 13:903758. <https://doi.org/10.3389/fimmu.2022.903758> PMID:36016939
 19. Xu C, Jia B, Yang Z, Han Z, Wang Z, Liu W, Cao Y, Chen Y, Gu J, Zhang Y. Integrative Analysis Identifies TCIRG1 as a Potential Prognostic and Immunotherapy-Relevant Biomarker Associated with Malignant Cell Migration in Clear Cell Renal Cell Carcinoma. *Cancers (Basel).* 2022; 14:4583. <https://doi.org/10.3390/cancers14194583> PMID:36230507
 20. Lu Q, Wang L, Gao Y, Zhu P, Li L, Wang X, Jin Y, Zhi X, Yu J, Li X, Qin X, Zhou P. lncRNA APOC1P1-3 promoting anoikis-resistance of breast cancer cells. *Cancer Cell Int.* 2021; 21:232. <https://doi.org/10.1186/s12935-021-01916-w> PMID:33902604
 21. Serghiou S, Kyriakopoulou A, Ioannidis JP. Long noncoding RNAs as novel predictors of survival in human cancer: a systematic review and meta-analysis. *Mol Cancer.* 2016; 15:50. <https://doi.org/10.1186/s12943-016-0535-1> PMID:27352941
 22. Liu J, Wu H, Gao Z, Lou M, Yuan K. Construction of an immune-related lncRNA pairs model to predict prognosis and immune landscape of lung adenocarcinoma patients. *Bioengineered.* 2021; 12:4123–35. <https://doi.org/10.1080/21655979.2021.1953215> PMID:34288805
 23. Zhou S, Cai Y, Xu Z, Peng B, Liang Q, Peng J, Yan Y. Identification of a pyroptosis-related lncRNA signature in the regulation of prognosis, metabolism signals and immune infiltration in lung adenocarcinoma. *Front Endocrinol (Lausanne).* 2022; 13:964362. <https://doi.org/10.3389/fendo.2022.964362>

- PMID:[36034461](#)
24. Zhao W, Wang J, Luo Q, Peng W, Li B, Wang L, Zhang C, Duan C. Identification of LINC02310 as an enhancer in lung adenocarcinoma and investigation of its regulatory network via comprehensive analyses. *BMC Med Genomics*. 2020; 13:185.
<https://doi.org/10.1186/s12920-020-00834-6>
PMID:[33308216](#)
 25. Parnigoni A, Caon I, Teo WX, Hua SH, Moretto P, Bartolini B, Viola M, Karousou E, Yip GW, Götte M, Heldin P, Passi A, Vigetti D. The natural antisense transcript HAS2-AS1 regulates breast cancer cells aggressiveness independently from hyaluronan metabolism. *Matrix Biol*. 2022; 109:140–61.
<https://doi.org/10.1016/j.matbio.2022.03.009>
PMID:[35395387](#)
 26. Cheng C, Ru P, Geng F, Liu J, Yoo JY, Wu X, Cheng X, Euthine V, Hu P, Guo JY, Lefai E, Kaur B, Nohturfft A, et al. Glucose-Mediated N-glycosylation of SCAP Is Essential for SREBP-1 Activation and Tumor Growth. *Cancer Cell*. 2015; 28:569–81.
<https://doi.org/10.1016/j.ccell.2015.09.021>
PMID:[26555173](#)
 27. Noronha A, Belugali Nataraj N, Lee JS, Zhitomirsky B, Oren Y, Oster S, Lindzen M, Mukherjee S, Will R, Ghosh S, Simoni-Nieves A, Verma A, Chatterjee R, et al. AXL and Error-Prone DNA Replication Confer Drug Resistance and Offer Strategies to Treat EGFR-Mutant Lung Cancer. *Cancer Discov*. 2022; 12:2666–83.
<https://doi.org/10.1158/2159-8290.CD-22-0111>
PMID:[35895872](#)
 28. Zhao B, Wu B, Feng N, Zhang X, Zhang X, Wei Y, Zhang W. Aging microenvironment and antitumor immunity for geriatric oncology: the landscape and future implications. *J Hematol Oncol*. 2023; 16:28.
<https://doi.org/10.1186/s13045-023-01426-4>
PMID:[36945046](#)
 29. Efremova M, Rieder D, Klepsch V, Charoentong P, Finotello F, Hackl H, Hermann-Kleiter N, Löwer M, Baier G, Krogdram A, Trajanoski Z. Targeting immune checkpoints potentiates immunoediting and changes the dynamics of tumor evolution. *Nat Commun*. 2018; 9:32.
<https://doi.org/10.1038/s41467-017-02424-0>
PMID:[29296022](#)
 30. Datar IJ, Hauc SC, Desai S, Gianino N, Henick B, Liu Y, Syrigos K, Rimm DL, Kavathas P, Ferrone S, Schalper KA. Spatial Analysis and Clinical Significance of HLA Class-I and Class-II Subunit Expression in Non-Small Cell Lung Cancer. *Clin Cancer Res*. 2021; 27:2837–47.
<https://doi.org/10.1158/1078-0432.CCR-20-3655>
PMID:[33602682](#)
 31. Jardim DL, Goodman A, de Melo Gagliato D, Kurzrock R. The Challenges of Tumor Mutational Burden as an Immunotherapy Biomarker. *Cancer Cell*. 2021; 39:154–73.
<https://doi.org/10.1016/j.ccell.2020.10.001>
PMID:[33125859](#)
 32. Hu J, Cao J, Topatana W, Juengpanich S, Li S, Zhang B, Shen J, Cai L, Cai X, Chen M. Targeting mutant p53 for cancer therapy: direct and indirect strategies. *J Hematol Oncol*. 2021; 14:157.
<https://doi.org/10.1186/s13045-021-01169-0>
PMID:[34583722](#)
 33. Jia Y, Duan Y, Liu T, Wang X, Lv W, Wang M, Wang J, Liu L. LncRNA TTN-AS1 promotes migration, invasion, and epithelial mesenchymal transition of lung adenocarcinoma via sponging miR-142-5p to regulate CDK5. *Cell Death Dis*. 2019; 10:573.
<https://doi.org/10.1038/s41419-019-1811-y>
PMID:[31363080](#)
 34. Offin M, Rizvi H, Tenet M, Ni A, Sanchez-Vega F, Li BT, Drilon A, Kris MG, Rudin CM, Schultz N, Arcila ME, Ladanyi M, Riely GJ, et al. Tumor Mutation Burden and Efficacy of EGFR-Tyrosine Kinase Inhibitors in Patients with EGFR-Mutant Lung Cancers. *Clin Cancer Res*. 2019; 25:1063–9.
<https://doi.org/10.1158/1078-0432.CCR-18-1102>
PMID:[30045933](#)
 35. Devarakonda S, Rotolo F, Tsao MS, Lanc I, Brambilla E, Masood A, Olaussen KA, Fulton R, Sakashita S, McLeer-Florin A, Ding K, Le Teuff G, Shepherd FA, et al. Tumor Mutation Burden as a Biomarker in Resected Non-Small-Cell Lung Cancer. *J Clin Oncol*. 2018; 36:2995–3006.
<https://doi.org/10.1200/JCO.2018.78.1963>
PMID:[30106638](#)
 36. Chan TA, Yarchoan M, Jaffee E, Swanton C, Quezada SA, Stenzinger A, Peters S. Development of tumor mutation burden as an immunotherapy biomarker: utility for the oncology clinic. *Ann Oncol*. 2019; 30:44–56.
<https://doi.org/10.1093/annonc/mdy495>
PMID:[30395155](#)
 37. Gui CP, Wei JH, Chen YH, Fu LM, Tang YM, Cao JZ, Chen W, Luo JH. A new thinking: extended application of genomic selection to screen multiomics data for development of novel hypoxia-immune biomarkers and target therapy of clear cell renal cell carcinoma. *Brief Bioinform*. 2021; 22:bbab173.
<https://doi.org/10.1093/bib/bbab173> PMID:[34237133](#)
 38. Hu FF, Liu CJ, Liu LL, Zhang Q, Guo AY. Expression profile of immune checkpoint genes and their roles in predicting immunotherapy response. *Brief Bioinform*. 2021; 22:bbaa176.

<https://doi.org/10.1093/bib/bbaa176>

PMID:[32814346](https://pubmed.ncbi.nlm.nih.gov/32814346/)

39. Wang Z, Wang Y, Yang T, Xing H, Wang Y, Gao L, Guo X, Xing B, Wang Y, Ma W. Machine learning revealed stemness features and a novel stemness-based

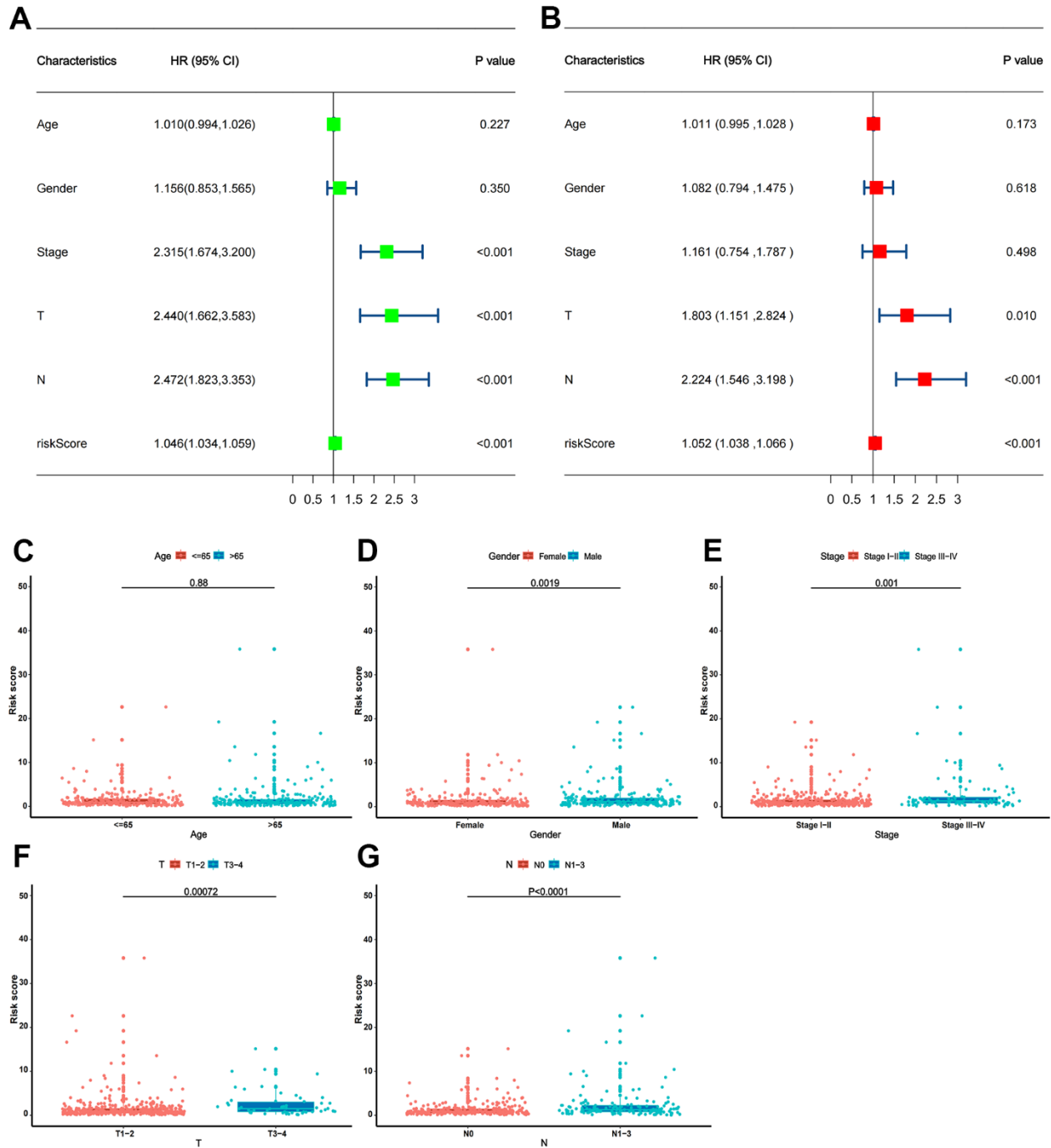
classification with appealing implications in discriminating the prognosis, immunotherapy and temozolomide responses of 906 glioblastoma patients. *Brief Bioinform.* 2021; 22:bbab032.

<https://doi.org/10.1093/bib/bbab032>

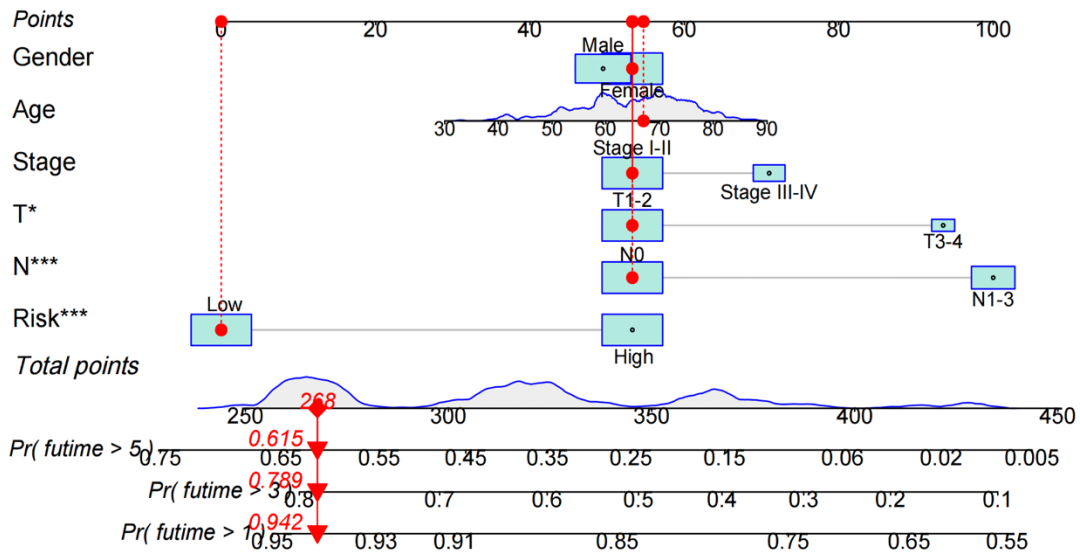
PMID:[33839757](https://pubmed.ncbi.nlm.nih.gov/33839757/)

SUPPLEMENTARY MATERIALS

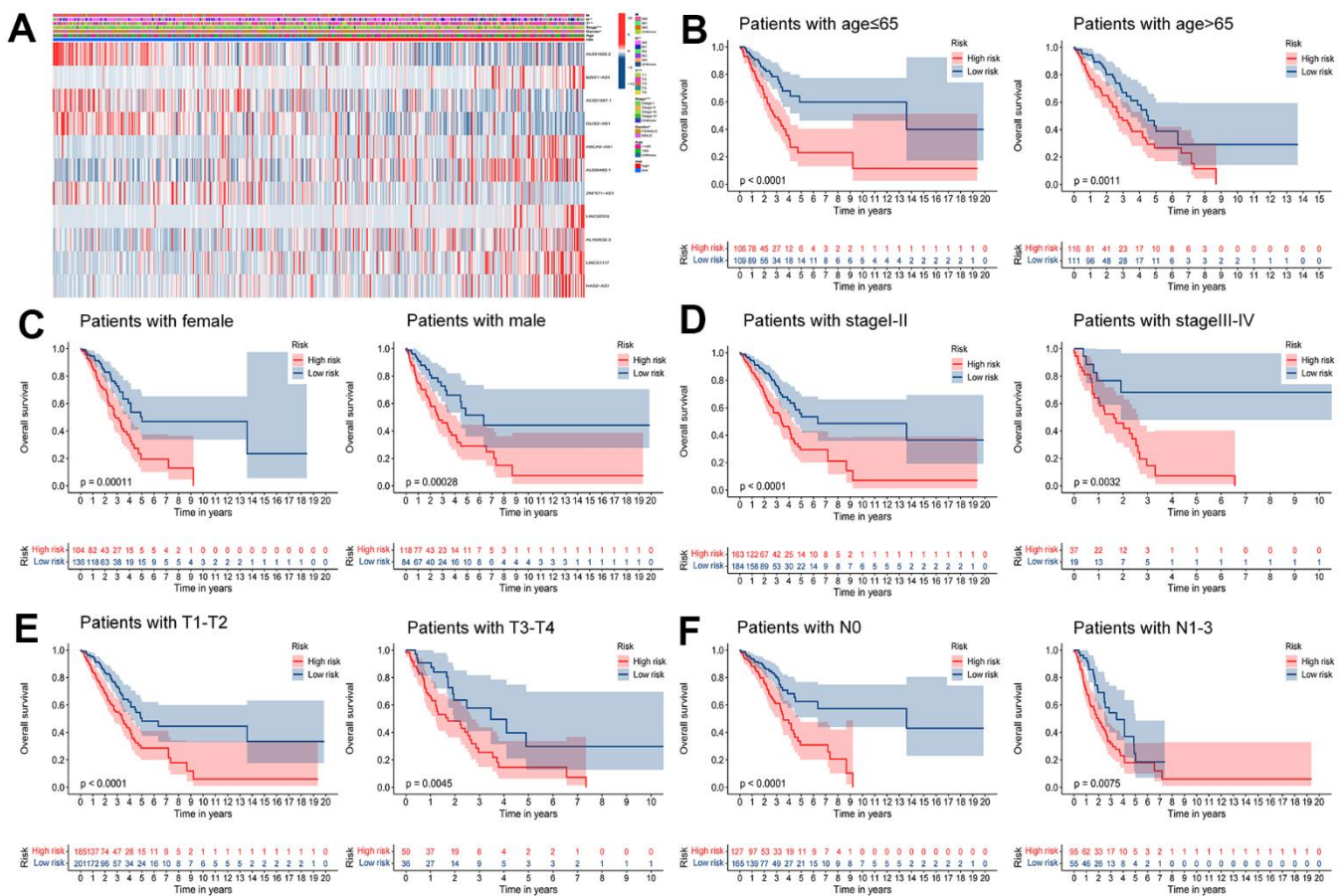
Supplementary Figures



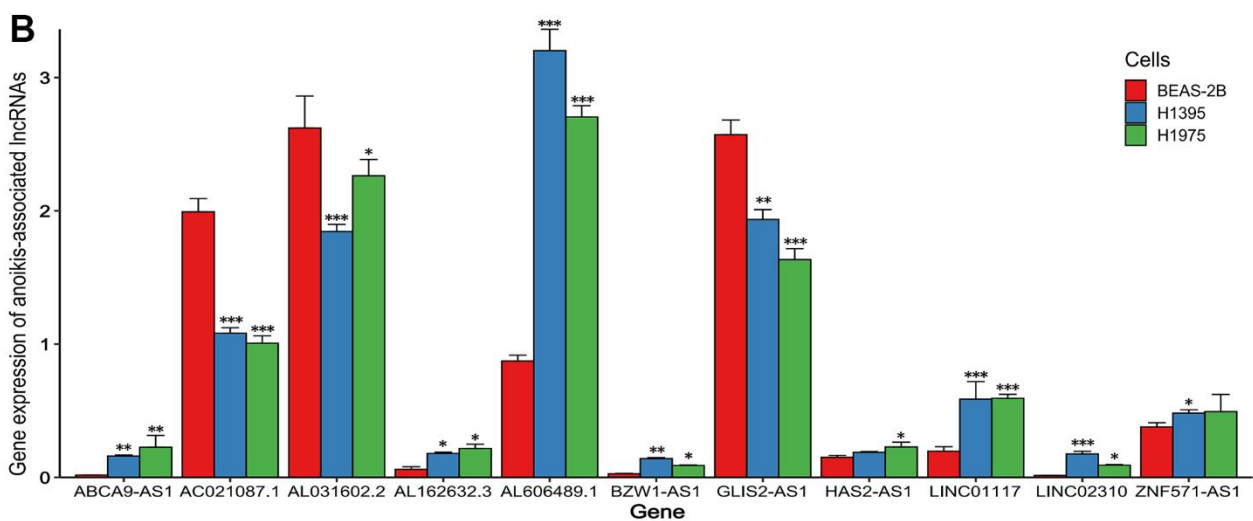
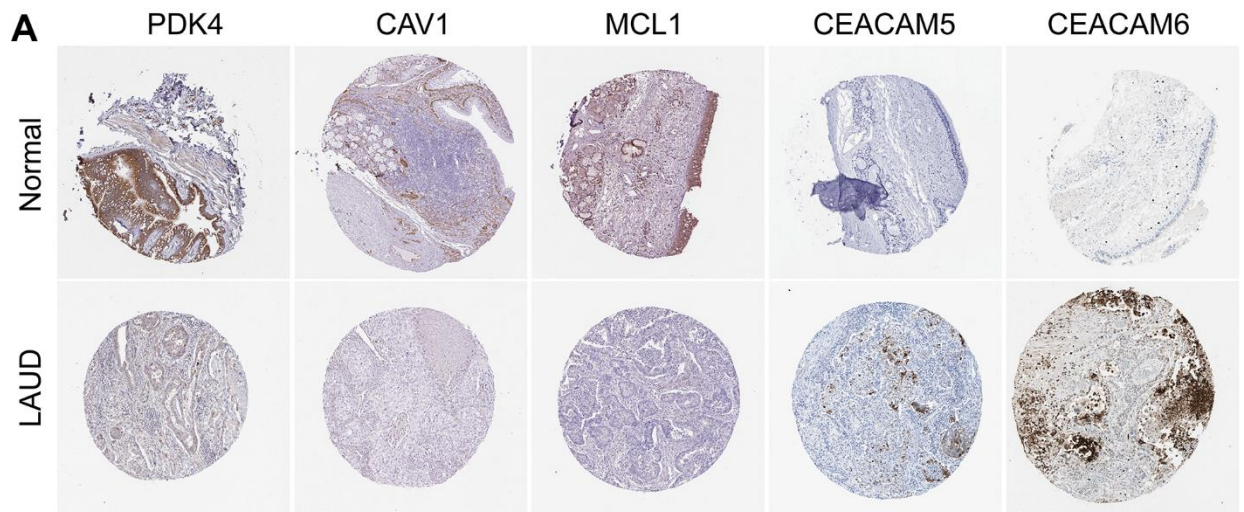
Supplementary Figure 1. Independent prognostic analysis of the prognostic signature. (A) Univariate and (B) Multivariate Cox regression analysis to examine the value of clinical characteristics and risk score as independent prognostic predictors. Correlation analysis of risk score with age (C), gender (D), stage (E), T stage (F) and N stage (G).



Supplementary Figure 2. Nomograms for predicting 1-, 3-, 5-year overall survival for a randomly selected patient in test cohort.



Supplementary Figure 3. Subgroup validation based on clinical features. (A) Heatmap for expression levels and correlation of risk signature with clinical factors. Kaplan-Meier survival analysis between high- and low-risk groups stratified by clinical characteristics: (B) age (≤ 65 and > 65), (C) gender (female and male), (D) stage (I-II and III-IV), (E) T stage (T1-2 and T3-4) and (F) N stage (N0 and N1-3).



Supplementary Figure 4. Validation of apoptosis-related genes and ARlncRNAs expression levels. (A) Protein expression map of the top 5 differential apoptosis-related genes in normal and tumor tissues. **(B)** Expression levels of 11 ARlncRNAs in high and low risk groups.

Supplementary Table

Please browse Full Text version to see the data of Supplementary Tables 4–6.

Supplementary Table 1. Primers for RT-qPCR experiments of 11 ARlncRNAs.

Gene	Forward primer	Reverse primer
AL031602.2	ATCTTCCCTGTCACCTCCCTT	CTGGGACATTCACACGGATG
BZW1-AS1	AGGACACAGGCCGAAGATTG	CACACTCGGGAGACAACCG
AC021087.1	CTCGAGCAGGGACGTATCAC	AAAGGGCAAGATAACGGCCA
GLIS2-AS1	TGCTAATTACTGCGGGGTCC	AAACTGAGGAACGGAAGGCTC
ABCA9-AS1	TCCAGTGTCTGCACCAGTT	TGGCCCAACGTCTAATAGGG
AL606489.1	TCCTTTATCGGGCAAGAGGC	TGGGTGCAATGAGAGTGCAT
ZNF571-AS1	CGCCATCCCCTTTTCCTCTT	CGGTCCAAAGGTTCTCCGAA
LINC02310	GGGATAAATCCTCCCTGCC	TCAGTTTTGCAGAAGGGGCT
AL162632.3	TGGCCGTAAAGTAAAACCCT	TCGGCCCAAAGGAGAAGAAA
LINC01117	CCCCGTGCTCGTTACAATCT	CTCCGGGGTTACTGGAGTCT
HAS2-AS1	CCCGTTCACCCCTCATAC	GAATTCGTCACGGCAGTTCC

Abbreviation: ARlncRNAs, anoikis-related lncRNAs; RT-qPCR, Reverse transcription quantitative-polymerase chain reaction.

Supplementary Table 2. The 148 ARlncRNAs connected with the over survival of the LUAD patients screened after univariate Cox analysis in training cohort (P<0.05).

Gene	HR	HR (95% CI)	P-value	Gene	HR	HR (95% CI)	P-value
MIR4435-2HG	1.68	(1.17,2.42)	0.005	AL445309.1	0.59	(0.39,0.91)	0.016
AC103681.2	0.29	(0.10,0.81)	0.018	AC092718.4	1.45	(1.15,1.85)	0.002
AC107308.1	1.30	(1.05,1.61)	0.016	Z97989.1	0.61	(0.38,0.98)	0.042
TSPOAP1-AS1	0.65	(0.44,0.98)	0.039	AC026356.1	1.34	(1.03,1.76)	0.030
AC039056.2	1.40	(1.05,1.88)	0.022	ABCA9-AS1	2.10	(1.14,3.87)	0.017
LINC01863	0.68	(0.48,0.96)	0.027	C2orf27A	1.50	(1.06,2.13)	0.023
CYP1B1-AS1	0.51	(0.27,0.96)	0.038	AC079313.2	2.46	(1.47,4.13)	0.001
AL109615.4	0.71	(0.54,0.94)	0.017	SMILR	1.60	(1.19,2.15)	0.002
AC087501.4	0.43	(0.25,0.75)	0.003	AC116407.1	0.80	(0.64,0.99)	0.045
AC092279.1	0.73	(0.56,0.96)	0.022	AC006116.9	0.21	(0.05,0.88)	0.033
AC022148.2	0.30	(0.10,0.90)	0.032	GMDS-DT	0.40	(0.20,0.80)	0.009
ZKSCAN7-AS1	0.59	(0.38,0.92)	0.021	LINC01116	1.28	(1.09,1.49)	0.002
AC009509.4	1.75	(1.17,2.63)	0.007	AC092574.1	0.65	(0.45,0.93)	0.020
CACTIN-AS1	2.48	(1.04,5.92)	0.041	AL606489.1	1.43	(1.16,1.77)	0.001
AC090948.1	0.72	(0.53,0.98)	0.034	DEPDC1-AS1	4.28	(1.89,9.66)	<0.001
AC090023.2	1.85	(1.24,2.75)	0.003	AL449423.1	1.67	(1.03,2.72)	0.037
LINC01138	1.42	(1.00,2.00)	0.047	AL691432.2	0.62	(0.47,0.84)	0.002
AC018529.1	0.58	(0.34,0.98)	0.042	ZNF571-AS1	0.63	(0.41,0.97)	0.035
AC011477.2	0.70	(0.54,0.92)	0.009	RASAL2-AS1	1.56	(1.01,2.40)	0.043
AC007552.2	0.77	(0.61,0.97)	0.024	AL157895.1	0.48	(0.25,0.94)	0.032
SH3BP5-AS1	0.75	(0.58,0.97)	0.027	AL358115.1	1.60	(1.03,2.49)	0.035
SNHG14	0.67	(0.45,0.99)	0.042	AC025171.2	0.74	(0.57,0.97)	0.029
APCDD1L-DT	1.53	(1.20,1.94)	0.001	AC112721.1	1.34	(1.01,1.77)	0.040
AC124242.1	0.51	(0.29,0.89)	0.019	DAAM2-AS1	0.40	(0.18,0.91)	0.029
AC027031.2	1.37	(1.09,1.72)	0.006	AC010615.2	0.79	(0.62,1.00)	0.047

CYTOR	1.62	(1.11,2.36)	0.013	TMEM30A-DT	0.27	(0.11,0.68)	0.006
ADAMTS9-AS2	0.47	(0.25,0.89)	0.020	AL137009.1	0.64	(0.43,0.94)	0.021
AC003991.1	0.57	(0.33,0.98)	0.041	AL359220.1	0.58	(0.36,0.93)	0.022
LINC00520	1.80	(1.20,2.69)	0.004	ZNF32-AS2	0.73	(0.54,0.99)	0.045
LINC00460	1.18	(1.02,1.37)	0.026	AC125807.2	1.33	(1.01,1.74)	0.041
AC107021.2	1.25	(1.00,1.57)	0.047	LINC02310	2.75	(1.83,4.14)	<0.001
AL008729.2	0.80	(0.66,0.97)	0.025	AC138965.1	1.63	(1.07,2.48)	0.023
AL031602.2	0.53	(0.36,0.78)	0.001	STXBP5-AS1	2.45	(1.11,5.42)	0.027
BZW1-AS1	2.43	(1.58,3.74)	<0.001	AC034223.2	1.53	(1.28,1.85)	<0.001
AC008937.3	0.46	(0.23,0.93)	0.030	AP005264.1	1.91	(1.21,3.03)	0.006
AC100810.3	1.68	(1.15,2.47)	0.007	AP005717.2	2.35	(1.01,5.48)	0.047
LINC02728	0.43	(0.21,0.90)	0.025	AC010343.3	1.54	(1.07,2.21)	0.019
AC092718.5	0.58	(0.38,0.91)	0.017	AC024075.1	0.76	(0.6,0.97)	0.025
AC021087.1	0.57	(0.38,0.84)	0.005	AL162632.3	2.96	(1.22,7.18)	0.016
AC084048.1	0.45	(0.21,0.97)	0.042	AC024075.3	0.72	(0.53,0.97)	0.031
AC004540.2	0.59	(0.37,0.94)	0.026	AC091057.1	1.35	(1.03,1.78)	0.030
AC021087.3	0.58	(0.37,0.93)	0.023	AC022210.1	1.53	(1.09,2.15)	0.013
AL137186.2	1.73	(1.04,2.86)	0.034	AC090409.1	1.88	(1.00,3.55)	0.050
GLIS2-AS1	0.62	(0.45,0.84)	0.002	ZNF790-AS1	0.62	(0.42,0.92)	0.017
LINC02848	0.06	(0.01,0.74)	0.028	AL356608.1	0.13	(0.03,0.56)	0.006
TMPO-AS1	1.38	(1.02,1.86)	0.034	LINC01117	1.88	(1.41,2.50)	<0.001
AL354953.1	1.31	(1.11,1.55)	0.002	AC008870.2	0.73	(0.53,0.99)	0.045
STEAP2-AS1	1.76	(1.13,2.73)	0.012	AC108136.1	1.97	(1.37,2.83)	<0.001
ZRANB2-AS2	0.17	(0.04,0.74)	0.018	AL353804.1	0.73	(0.56,0.96)	0.026
AC091435.2	0.61	(0.38,0.99)	0.047	AL139351.3	1.77	(1.23,2.55)	0.002
AC124045.1	0.67	(0.46,1.00)	0.048	ASB16-AS1	0.69	(0.47,0.99)	0.046
RMDN2-AS1	0.58	(0.35,0.96)	0.034	LINC01537	2.40	(1.60,3.60)	<0.001
AP000864.1	2.22	(1.11,4.43)	0.024	AC006058.3	1.57	(1.15,2.16)	0.005
AC026355.2	0.81	(0.67,0.98)	0.034	AC123595.2	0.61	(0.41,0.90)	0.014
AC092640.1	1.94	(1.12,3.36)	0.018	AC005865.2	1.40	(1.05,1.88)	0.024
AL138689.1	1.37	(1.06,1.77)	0.018	HAS2-AS1	5.20	(2.48,10.92)	<0.001
AC084781.1	2.79	(1.20,6.47)	0.017	AC092329.4	0.53	(0.33,0.87)	0.011
AL031778.1	0.64	(0.44,0.92)	0.017	AP000695.1	1.53	(1.23,1.91)	<0.001
AP000695.2	1.48	(1.16,1.88)	0.001	AL138921.2	0.66	(0.44,0.98)	0.039
AC135050.6	0.60	(0.44,0.82)	0.001	AL138789.1	1.53	(1.15,2.02)	0.003
AL109811.2	0.61	(0.44,0.84)	0.003	AC025419.1	1.51	(1.15,1.98)	0.003
LINC01711	1.40	(1.13,1.74)	0.002	AC024909.1	0.61	(0.38,0.98)	0.041
TRMT2B-AS1	0.56	(0.34,0.94)	0.028	AC068580.2	1.41	(1.00,1.98)	0.047
MANCR	1.68	(1.34,2.10)	<0.001	AL355075.2	0.76	(0.59,0.98)	0.035
AL139424.3	0.42	(0.18,0.95)	0.037	NAGPA-AS1	0.64	(0.42,0.98)	0.042
AC127024.5	0.69	(0.50,0.97)	0.030	HCG18	0.53	(0.34,0.85)	0.007
AL158068.2	1.95	(1.02,3.70)	0.042	AL391261.1	2.08	(1.33,3.26)	0.001
NIPBL-DT	0.69	(0.50,0.95)	0.023	MAP3K4-AS1	1.55	(1.09,2.21)	0.016
AC016735.1	1.37	(1.03,1.82)	0.030	AL359643.2	0.26	(0.08,0.91)	0.035
AC019205.1	0.56	(0.32,0.97)	0.038	AC114781.2	0.45	(0.24,0.84)	0.013
LINC01385	1.33	(1.03,1.72)	0.029	AC060780.1	0.70	(0.50,0.97)	0.033
AC034102.8	0.62	(0.41,0.92)	0.019	AL590729.1	0.57	(0.35,0.92)	0.022
DIRC3	2.27	(1.20,4.30)	0.012	SEPSECS-AS1	0.62	(0.39,0.99)	0.045
MIR31HG	1.54	(1.30,1.81)	<0.001	LINC02582	1.41	(1.11,1.78)	0.005

Abbreviation: ARlncRNAs, anoikis-related lncRNAs; CI, Confidence interval; HR, Hazard ratios; LUAD, Lung adenocarcinoma.

Supplementary Table 3. 11 ARlncRNAs connected with the over survival of the LUAD patients after multivariate Cox analysis in training cohort.

Gene	HR	HR (95% CI)	Coef	P-value
AL031602.2	0.49	(0.32,0.77)	-0.710450178205890	0.002
BZW1-AS1	1.54	(0.93,2.54)	0.432038348321673	0.092
AC021087.1	0.62	(0.41,0.94)	-0.476411291926875	0.025
GLIS2-AS1	0.64	(0.46,0.87)	-0.454008732783369	0.005
ABCA9-AS1	2.72	(1.31,5.63)	0.999706491359515	0.007
AL606489.1	1.30	(1.03,1.63)	0.259835252523394	0.025
ZNF571-AS1	0.71	(0.44,1.12)	-0.348748604018090	0.139
LINC02310	2.12	(1.24,3.62)	0.750892025449650	0.006
AL162632.3	3.73	(1.43,9.72)	1.315573571091090	0.007
LINC01117	1.40	(1.03,1.90)	0.338762422003907	0.029
HAS2-AS1	2.17	(0.93,5.05)	0.775846321855369	0.072

Abbreviations: ARlncRNAs, anoikis-related lncRNAs; CI, Confidence interval; Coef, Coefficient; HR, Hazard ratios; LUAD, Lung adenocarcinoma.

Supplementary Table 4. The risk scores and risk groups of LUAD patients in the total cohort.

Supplementary Table 5. The risk scores and risk groups of LUAD patients in the training cohort.

Supplementary Table 6. The risk scores and risk groups of LUAD patients in the test cohort.

Supplementary Table 7. The 6 sensitive drugs in the low-risk group were obtained by chemotherapy drug sensitivity analysis at P<0.001.

Drug	P-value	L.median (25%,75%)	H.median (25%,75%)
IGF1R signaling			
BMS-754807_2171	<0.001	1.4(0.46-2.80)	2.29(0.87-4.24)
JNK and p38 signaling			
Doramapimod_1042	<0.001	83.61(69.75-104.75)	102.35(79.12-125.55)
Mitosis			
ZM447439_1050	<0.001	16.88(14.01-22.23)	19.95(15.60-27.00)
SB505124_1194	<0.001	9.81(7.58-11.49)	10.55(8.91-12.46)
PI3K/MTOR signaling			
PF-4708671_1129	<0.001	44.12(35.94-56.42)	52.27(40.16-67.21)
RTK signaling			
Axitinib_1021	<0.001	19.84(15.40-25.53)	24.51(19.14-31.54)

Abbreviation: H, High risk group; L, Low risk group.

Supplementary Table 8. The 59 sensitive drugs in the high-risk group were obtained by chemotherapy drug sensitivity analysis at P<0.001.

Drug	P-value	L.median (25%,75%)	H.median (25%,75%)
Apoptosis regulation			
Wee1 Inhibitor_1046	<0.001	7.47(3.92-17.87)	5.43(2.84-9.77)
PD0325901_1060	<0.001	1.81(1.13-3.32)	1.32(0.75-2.20)
IAP_5620_1428	0.001	166.18(101.98-300.14)	132.62(73.47-237.21)
Vinorelbine_2048	<0.001	0.04(0.02-0.16)	0.02(0.01-0.08)
Apoptosis regulation			
Palbociclib_1054	0.001	43.51(27.37-73.12)	34.73(21.48-54.85)
BI-2536_1086	0.001	1.52(0.97-2.46)	1.25(0.63-2.04)
MK-1775_1179	<0.001	1.81(0.98-4.43)	1.03(0.60-2.06)
VE821_2111	<0.001	60.1(34.42-139.30)	36.68(21.63-75.00)
Chromatin other			
MK-8776_2046	<0.001	24.11(12.15-59.18)	12.82(7.41-25.27)
DNA replication			
Gemcitabine_1190	0.001	0.6(0.21-1.62)	0.37(0.14-1.06)
Epirubicin_1511	0.001	0.36(0.20-0.76)	0.27(0.16-0.52)
Foretinib_2040	<0.001	2.61(1.44-4.64)	1.68(0.96-2.93)
Pyridostatin_2044	0.001	25.58(15.86-47.59)	20.14(13.58-35.02)
EGFR signaling			
Gefitinib_1010	<0.001	23.98(14.81-43.06)	17.29(11.02-32.56)
Erlotinib_1168	<0.001	13.92(9.28-22.93)	10.35(6.73-17.11)
Lapatinib_1558	0.001	19.14(9.89-42.41)	13.51(7.37-29.66)
AZD3759_1915	<0.001	13.02(8.81-23.27)	10.95(7.05-17.85)
Ulixertinib_2047	<0.001	9.95(5.74-16.58)	8.51(5.34-12.73)
ERK MAPK signaling			
Alisertib_1051	0.001	6.34(2.64-20.79)	4.51(1.84-10.41)
Trametinib_1372	<0.001	2.18(1.07-4.93)	1.23(0.52-3.19)
VE-822_1613	<0.001	30.55(14.81-75.84)	18.45(9.74-44.10)
ERK_6604_1714	<0.001	36.5(22.63-62.14)	28.49(15.34-48.95)
AZD4547_1786	<0.001	18(10.57-33.60)	13.67(8.02-21.89)
Buparlisib_1873	<0.001	2.47(1.77-4.16)	1.96(1.38-3.24)
Genome integrity			
Vinblastine_1004	<0.001	0.02(0.01-0.08)	0.02(0.01-0.04)
Talazoparib_1259	<0.001	28.19(15.37-52.10)	18.24(9.69-33.86)
Pevonedistat_1529	<0.001	2.1(1.02-5.31)	1.4(0.58-2.92)
Hormone-related			
Fulvestrant_1200	<0.001	16.13(10.95-29.25)	12.87(9.41-19.21)
GDC0810_1925	<0.001	129.24(93.10-205.90)	98.57(71.36-156.54)
IGF1R signaling			
AZD7762_1022	<0.001	1.03(0.58-2.41)	0.67(0.38-1.23)
Staurosporine_1034	<0.001	0.05(0.03-0.11)	0.03(0.02-0.06)
Metabolism			
GSK2606414_1618	0.001	38.55(24.86-64.48)	32.2(22.40-46.59)
Mitosis			
Cisplatin_1005	<0.001	30.97(14.04-72.36)	14.26(5.53-34.88)
Docetaxel_1007	<0.001	0.01(0.01-0.03)	0.01(0.00-0.01)
Luminespib_1559	<0.001	0.1(0.05-0.27)	0.07(0.04-0.14)
Savolitinib_1936	<0.001	14.36(7.64-26.69)	8.08(4.85-13.45)

p53 pathway			
MIRA-1_1931	<0.001	196.28(107.82-367.99)	147.05(94.10-247.43)
PI3K/MTOR signaling			
Dactolisib_1057	<0.001	0.19(0.11-0.37)	0.14(0.08-0.26)
GNE-317_1926	<0.001	1.74(0.99-3.40)	1.17(0.76-2.24)
Ipatasertib_1924	0.001	27.69(14.41-62.63)	21.89(11.05-40.65)
LJI308_2107	0.001	166.78(102.37-296.89)	124.37(77.98-205.04)
Pictilisib_1058	<0.001	3.92(2.19-8.61)	2.71(1.59-5.31)
Taselisib_1561	<0.001	9.15(4.13-19.07)	5.97(2.48-14.13)
Paclitaxel_1080	<0.001	0.07(0.03-0.24)	0.04(0.02-0.10)
YK-4-279_1239	<0.001	9.56(4.99-26.66)	6.15(3.26-14.90)
Alpelisib_1560	<0.001	36.02(17.94-77.46)	22.27(10.47-47.92)
AMG-319_2045	<0.001	115.83(75.92-196.16)	92.09(61.12-149.61)
AT13148_2170	0.001	30.38(17.05-72.24)	21.85(12.17-55.76)
Protein stability and degradation			
BMS-536924_1091	<0.001	9.14(5.90-13.51)	6.47(4.29-10.45)
BPD-00008900_1998	<0.001	91.93(63.06-146.75)	69.9(47.88-112.14)
RTK signaling			
5-Fluorouracil_1073	<0.001	123.65(55.68-338.28)	63.96(25.47-183.49)
Other			
Cytarabine_1006	<0.001	6.77(3.12-13.02)	4.26(1.83-8.59)
Dasatinib_1079	<0.001	5.49(2.05-17.88)	3.47(0.70-11.36)
Dabrafenib_1373	0.001	101.23(54.01-186.31)	74.25(34.06-145.65)
Temozolomide_1375	<0.001	328.03(226.50-763.95)	274.93(162.41-466.20)
I-BET-762_1624	<0.001	29.3(19.04-47.07)	21.97(14.31-37.35)
AZD6738_1917	<0.001	8.84(4.63-20.71)	5.38(2.63-9.13)
VX-11e_2096	<0.001	18.18(12.24-34.21)	12.77(7.66-21.69)
Unclassified			
BDP-00009066_1866	<0.001	9.61(7.16-17.15)	8.07(5.66-11.79)

Abbreviation: H, High risk group; L, Low risk group.